JCTC Journal of Chemical Theory and Computation

Article

pubs.acs.org/JCTC

Density Functional Theory of Open-Shell Systems. The 3d-Series Transition-Metal Atoms and Their Cations

Sijie Luo, Boris Averkiev,† Ke R. Yang, Xuefei Xu, and Donald G. Truhlar*

Department of Chemistry and Supercomputing Institute, University of Minnesota, Minneapolis, Minnesota 55455-0431, United States

ABSTRACT: The 3d-series transition metals (also called the fourth-period transition metals), Sc to Zn, are very important in industry and biology, but they provide unique challenges to computing the electronic structure of their compounds. In order to successfully describe the compounds by theory, one must be able to describe their components, in particular the constituent atoms and cations. In order to understand the ingredients required for successful computations with density functional theory, it is useful to examine the performance of various exchange−correlation functionals; we do this here for $4s^N3d^{N'}$ transition-metal atoms and their cations. We analyze the results using three ways to compute the energy of the open-shell states: the direct variational method, the weighted-averaged broken symmetry (WABS) method, and a new broken-symmetry method called the reinterpreted broken symmetry (RBS) method. We find the RBS method to be comparable in accuracy with the WABS method. By examining the overall accuracy in treating 18 multiplicity-changing excitations and 10 ionization potentials with the RBS method, 10 functionals are found to have a mean-unsigned error of <5 kcal/mol, with ωB97X-D topping the list. For local density functionals, which are more practical for extended systems, the M06-L functional is the most accurate. And by combining the results with our previous studies of p-block and 4d-series elements as well as databases for alkyl bond dissociation, main-group atomization energies, and π−π noncovalent interactions, we find five functionals, namely, PW6B95, MPW1B95, M08-SO, SOGGA11-X, and MPWB1K, to be highly recommended. We also studied the performance of PW86 and C09 exchange functionals, which have drawn wide interest in recent studies due to their claimed ability to reproduce Hartree−Fock exchange at long distance. By combining them with four correlation functionals, we find the performance of the resulting functionals disappointing both for 3d transition-metal chemistry and in broader tests, and thus we do not recommend PW86 and C09 as components of generalized gradient approximations for general application.

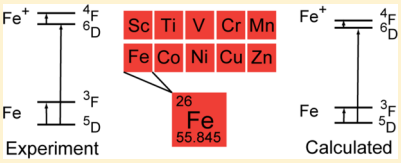

1. INTRODUCTION

Many systems involving transition-metal atoms have open-shell electronic structures with several low-energy states differing in spin and/or in orbital occupancy. It is common practice to apply Kohn−Sham (KS) density functional theory (DFT)[1] to the lowest-energy state of each total electronic spin component (M_S),[2,3] to identify the ground state, and to model the properties, spectra, and reactivity of each spin state. However, when $2M_S$ is less than the number n_{SO} of singly occupied orbitals, the state is intrinsically multideterminental, and one finds that KS-DFT, with its single-determinantal noninteracting reference state for computing the dominant portion of the kinetic energy, is often less accurate for the low-spin open-shell states than for the high-spin and closed-shell states ($M_S = n_{SO}/2$) for which a single Slater determinant is a good reference function. This is mainly due to the fact that presently available exchange−correlation (xc) functionals, which are the only approximations in KS-DFT, usually cannot treat the multi-reference systems and single-reference ones equally well.[2−4] The difficulty is compounded when the different spin states differ in their s and d occupancies (e.g., $ns^N(n-1)d^{N'}$ in one spin state and $ns^{N-1}(n-1)d^{N'+1}$ in the other), since the approximate xc functionals may have different accuracies for ns electrons than for $(n-1)$d electrons, which tend to be closer to the nucleus in a region of higher electron density. For the reasons above, it is worthwhile to test currently available xc functionals' performance in these difficult cases.

Testing the functionals requires care to be sure that the conclusions are not clouded by the following complications: (a) incomplete basis sets or inadequate effective core potentials; (b) incomplete treatment of relativistic effects, including spin−orbit coupling; (c) errors in reference data; and (d) cancellation of errors in treating the transition metal with errors in treating ligands or the ligand field exerted on the transition-metal site.

All of these possible complications are minimized or even eliminated by studying unligated atoms M and monatomic cations M^+ of the 3d-series. In particular, because these systems are small, one can afford to use nearly complete all-electron basis sets without effective core potentials. Also, the experimental excitation energies and ionization potentials are well established. Furthermore, the relativistic effects are small enough that Douglas−Kroll−Hess (DKH) second-order calculations should account well for scalar relativistic effects, and spin−orbit effects can be largely removed from experiment by considering the weighted average of the configuration. Finally, by studying atoms and monatomic ions, the treatment of electronic structure is decoupled from geometry optimiza-

Received: August 9, 2013

   dx.doi.org/10.1021/ct400712k | J. Chem. Theory Comput. XXXX, XXX, XXX−XXX

Table 1. Experimental Data[a]

	GS	ES	ΔE		GS^+	ES^+	ΔE^+	IP
Sc	^2D, $4s^23d^1$	^4F, $4s^13d^2$	32.9	Sc^+	^3D, $4s^13d^1$	^1D, $4s^13d^1$	7.0	151.3
Ti	^3F, $4s^23d^2$	^5F, $4s^13d^3$	18.6	Ti^+	^4F, $4s^13d^2$	^2F, $4s^13d^2$	13.0	157.6
V	^4F, $4s^23d^3$	^6D, $4s^13d^4$	5.6	V^+	^5D, $3d^4$	^3F, $4s^13d^3$	24.9	155.1
Cr	^7S, $4s^13d^5$	^5S, $4s^13d^5$	21.7	Cr^+	^6S, $3d^5$	^4D, $4s^13d^4$	56.7	156.0
Mn	^6S, $4s^23d^5$	^8P, $4s^13d^54p^1$	53.1	Mn^+	^7S, $4s^13d^5$	^5S, $4s^13d^5$	27.1	171.4
Fe	^5D, $4s^23d^6$	^3F, $4s^13d^7$	34.3	Fe^+	^6D, $4s^13d^6$	^4F, $3d^7$	5.7	182.2
Co	^4F, $4s^23d^7$	^2F, $4s^13d^8$	20.3	Co^+	^3F, $3d^8$	^5F, $4s^13d^7$	9.9	181.1
Ni	^3F, $4s^23d^8$	^1D, $4s^13d^9$	7.0	Ni^+	^2D, $3d^9$	^4F, $4s^13d^8$	25.0	175.0
Cu	^2S, $4s^13d^{10}$	^4P, $4s^13d^94p^1$	113.5	Cu^+	^1S, $3d^{10}$	^3D, $4s^13d^9$	64.8	178.2
Zn	^1S, $4s^23d^{10}$	^3P, $4s^13d^{10}4p^1$	93.5	Zn^+	^2S, $4s^13d^{10}$	^4P, $4s^13d^94p^1$	299.4	216.6

[a]GS − electronic state of neutral ground state; ES − electronic state of neutral excited state; ΔE − excitation energy of neutral atom, kcal/mol; GS^+ − electronic state of cation ground state; ES^+ − electronic state of cation excited state; ΔE^+ − excitation energy of cation, kcal/mol; IP − ionization potential, kcal/mol

tion, which can have a pronounced effect on such comparisons for molecules.

Thus in this article we present a systematic study of the ability of currently available xc functionals to predict the spin-transition excitation energies of all 3d-series transition-metal atoms (Sc through Zn) and their singly charged cations (Sc^+ through Zn^+) as well as the ionization potentials connecting these two sets. The treatment of open-shell systems by KS-DFT or its generalizations is an important frontier area of practical work in DFT. The 3d transition-metal series, because of its higher natural abundance than the other transition series, is very important for catalysis, including organometallic, heterogeneous, and biological catalysts.

In a certain sense, this paper is the third in a series, following up on closely related work on p-block atoms[5] and 4d-series atoms and ions.[6] Atoms and monatomic ions often have more near degeneracy character than catalytically important complexes with higher metal coordination numbers, and this can make them even more difficult to treat than the difficult transition-metal compounds; in this sense, these tests on atoms are not only of fundamental interest but also of interest in that they provide especially difficult challenges for DFT.

2. CALCULATION DETAILS AND EXPERIMENTAL DATA

All calculations were done with a locally modified version of *Gaussian 09*.[7] The integration grid for density functional calculations is a pruned grid obtained with 99 radial and 590 angular points, which is denoted as "ultrafine" in *Gaussian 09*. The all-electron relativistic cc-pVQZ-DK basis set was used,[8] and the scalar relativistic effect was included by using the DKH second-order scalar relativistic Hamiltonian.[9−11] To calculate 4s and 3d subshell occupation numbers for interpretation purposes, natural bond orbital (NBO) analysis[12−19] was performed using the NBO 3.1 package with *Gaussian 09*.

The experimental data were obtained from NBS tables.[20] For each experimental multiplet, the energy was averaged over the total angular momentum quantum number J; the $(2J + 1)$ degeneracy of each term was taken into account with the degeneracy-weighted average formula

$$\overline{E}(^{2S+1}L) = \frac{\sum_{J=|L-S|}^{L+S}(2J+1)E(^{2S+1}L_J)}{\sum_{J=|L-S|}^{L+S}(2J+1)} \quad (1)$$

Note that experimental S and L values are only nominal because S and L are not good quantum numbers. Since the spin−orbit operator is traceless, spin−orbit coupling does not change $\overline{E}$ to first order, and therefore $\overline{E}$ may be interpreted as an atomic energy in the absence of spin−orbit coupling (i.e., an atomic energy from which spin−orbit coupling has been removed). Although eq 1 is written in the Russell−Saunders coupling scheme, a degeneracy-weighted average also removes spin−orbit effects to first order when the coupling scheme is better described as j−j coupling. For our comparisons of theory to experiment, we compare calculations without spin−orbit coupling to experimental values obtained using degeneracy-weighted averages.

We label $\overline{E}$ of the ground state as E(GS). The excited state of interest in this paper is the lowest-energy excited state (ES) that has an S value different from the ground state (GS). The $\overline{E}$ of this state is called E(ES). Table 1 lists the excitation energies defined as

$$\Delta E = E(\mathrm{ES}) - E(\mathrm{GS}) \quad (2)$$

The energies and excitation energies for singly charged cations are labeled $E(GS^+)$, $E(ES^+)$, and ΔE^+. The ionization potential (IP) is

$$\mathrm{IP} = E(\mathrm{GS}^+) - E(\mathrm{GS}) \quad (3)$$

Table 1 also lists $2S + 1$, L, and the electron configuration of the GS and ES of each neutral atom and cation as well as ΔE, ΔE^+, and IP.

3. DENSITY FUNCTIONALS TESTED

We tested 75 xc functionals as well as the Hartree−Fock[21−23] method. In a general way, xc functionals may be divided into two groups: hybrid, in which some local exchange is replaced by a percentage X of nonlocal Hartree−Fock exchange, and local, in which the xc functional depends only on local variables, in particular on the local values of spin-labeled electron density, ρ_σ, where σ is α or β, and optionally also on the local values of the square of the reduced density gradient,[24] s^2_σ, which is defined as $|\nabla\rho_\sigma|^2/\rho_\sigma^{8/3}$, and on the local values of the spin-labeled kinetic energy densities τ_α and τ_β.

None of the xc functionals tested here has nonlocal correlation; therefore they may be divided into two general categories: local and hybrid, where the latter refers to a nonlocal functional in which the nonlocality is limited to including some Hartree−Fock nonlocal exchange. The xc

dx.doi.org/10.1021/ct400712k | J. Chem. Theory Comput. XXXX, XXX, XXX−XXX

Table 2. Various Exchange−Correlation Functionals Tested in this Work

type	xcF	X^a	ref
LSDA	GVWN3[b]	0	25,26
GGA	B88	0	27
	BP86	0	27, 28
	BLYP	0	27, 29
	PW91	0	30
	BPW91	0	27, 30
	PBE	0	31
	mPWLYP	0	29, 32
	HCTH	0	33, 34
	RPBE	0	35
	OLYP	0	29, 36
	OPBE	0	31, 36
	MOHLYP	0	37
	OreLYP	0	38
	SOGGA	0	43
	SOGGA11	0	45
	PW86LYP	0	29, 106
	PW86PBE	0	31, 106
	PW86reLYP	0	38, 106
	C09LYP	0	29, 107
	C09PBE	0	31, 107
	C09reLYP	0	38, 107
	PW86SOGGA11	0	45, 106
	C09SOGGA11	0	45, 107
NGA	N12	0	39
meta-GGA	VS98	0	40
	TPSS	0	41
	τHCTH	0	68
	M06-L	0	42
	revTPSS	0	44
range-separated meta-GGA	M11-L	0	46
meta-NGA	MN12-L	0	47
global-hybrid GGA	MPWLYP1M	5	37
	O3LYP	11.61	48
	B3LYP*	15	49
	B3PW91	20	50
	B3LYP	20	51
	B3V5LYP	20	52
	MPW3LYP	21.8	53
	B98	21.98	54
	PBE0	25	55
	B1LYP	25	56
	B97-1	21	57
	B97-2	21	58
	B97-3	26.93	59
	SOGGA11-X	40.15	60
	MPW1K	42.8	61
	MPW1B95	31	62
	MPWB1K	44	62
	BHandH	50	63
	BHandHLYP	50	29, 63
	HFLYP	100	29
	HFPW91	100	30
global-hybrid meta-GGA	TPSSh	10	64
	TPSS1KCIS	13	65−67
	τHCTHhyb	15	68
	M06	27	67, 69
	M05	28	66
	PW6B95	28	72
	MPWKCIS1K	41	32, 66, 73
	BMK	42	74
	M08-SO	52.23	75
	M06-2X	54	69, 70
	M05-2X	56	70, 75
	M08-HX	56.79	75
	M06-HF	100	77
screened-exchange GGA	HSE	0−25	78, 79
long-range-corrected GGA	CAM-B3LYP	19−65	80
	LC-MPWLYP	0−100	81
	LC-ωPBE	0−100	82
	ωB97X	15.77−100	83
screened-exchange NGA	N12-SX	0−25	85
long-range-corrected meta-GGA	M11	42.8−100	86
screened-exchange meta-NGA	MN12-SX	0−25	85
long-range-corrected GGA + MM	ωB97X-D	22.2−100	84

[a]For hybrid functionals that are not global hybrids, the first number is X at short-range, and the second is X at long-range. [b]GVWN3 denotes the combination of the Gáspár exchange functional (also used by Kohn and Sham and sometimes called GKS) with the third approximation of Vosko, Wilk, and Nusair for the correlation functional. The GVWN3 functional has the keyword SVWN in *Gaussian 09* and it is one of many (fairly similar) approximations in the generic class of LSDA functionals. We note that the Gáspár exchange functional is the same as Slater's Xα functional if the parameter α is set equal to 2/3.

functionals are listed in Table 2, where they are divided into the two categories and into 14 subtypes as in the following subsections.

Local Exchange−Correlation Functionals.

- Local spin-density approximation (LSDA): a functional that depends only on ρ_σ (for closed shells, this is sometimes called LDA).
- Generalized gradient approximation (GGA): a functional that also depends on s_σ^2, with the separability requirement that the exchange functional for each spin component σ is expressed as a product of a function of ρ_σ times a function of s_σ^2 (the correlation functional also depends only on ρ_σ and s_σ^2).
- Nonseparable gradient approximation (NGA): a functional that depends on the same variables as a GGA but without the separability requirement.
- meta-GGA: a functional like a GGA but that also depends on spin-labeled kinetic energy densities τ_α and τ_β.
- Range-separated meta-GGA: a functional like a meta-GGA but the parameters of the functional depend on interelectronic separation.
- meta-NGA: a functional like an NGA but that also depends on τ_α and τ_β.

Hybrid Exchange−Correlation Functionals.

- Global-hybrid GGA: a hybrid GGA where the percentage X of local exchange that is replaced by Hartree−Fock

dx.doi.org/10.1021/ct400712k | J. Chem. Theory Comput. XXXX, XXX, XXX−XXX

exchange is a global constant, i.e., it is independent of point in space, ρ_σ, $\nabla\rho_\sigma$, τ_σ, or interelectronic separation.
- Global-hybrid meta-GGA: a hybrid meta-GGA where the percentage X of local exchange that is replaced by Hartree−Fock exchange is a global constant.
- Long-range-corrected GGA: a hybrid GGA in which X increases as a function of interelectronic separation.
- Long-range-corrected meta-GGA: a hybrid meta-GGA in which X increases as a function of interelectronic separation.
- Screened exchange GGA: a hybrid GGA in which X decreases to zero as interelectronic separation increase.
- Screened exchange NGA: a hybrid NGA in which X decreases to zero as interelectronic separation increases.
- Screened exchange meta-NGA: like a screened-exchange NGA except the local part also depends on τ_α and τ_β (same as a long-range-corrected hybrid meta-GGA but using a meta-NGA rather than a meta-GGA, and X decreases rather than increases with interelectronic separation).
- Long-range-corrected GGA plus molecular mechanics: a hybrid GGA in which X increases as a function of interelectronic separation, and the functional includes a post-SCF molecular mechanics (MM) term.

Table 1 also shows the percentage of Hartree−Fock exchange X and gives the references[25−86] for each functional. Further details of the functional forms of the subtypes and the individual functionals may be found in these references. Many of the functionals are also discussed in more detail in refs 5 and 6; we simply note here that the functionals chosen for study in the present article are selected for various reasons, including their popularity, their good performance for one or another property in previous work, and their interest from a fundamental point of view.

We note one important point about the tests in the present article and most of the other tests and validation studies carried out in our group. Unlike most such tests, the list of xc functionals studied is not limited to those found in any single program. No single available software package has all the functionals studied in this paper. As just one example, the relatively recent OreLYP is not found in any software package that we know of, but we have coded this and other xc functionals for a local version of *Gaussian 09* to make our study more comprehensive.

Finally, we comment on the motivation for a group of eight new functionals tested here. Recently there has been extensive interest in designing better xc functionals for van der Waals interactions, and some studies have pointed to PW86,[106] a GGA exchange functional developed in the pioneering days of functional development, and C09,[107] a very recent GGA exchange functional, for their performance in conjunction with nonlocal correlation functionals.[108−110] These functionals apparently benefit from a reduced dependence on the density gradient for small values of the magnitude of the density gradient—thus either restoring the density gradient expansion through second order, as is done in the SOGGA[43] and SOGGA11[45] functionals, or nearly restoring it. With these functionals garnering attention, it is worthwhile to test their ability for application to general problems in chemistry. In this study we combine them with four correlation functionals for comprehensive evaluation, in particular with the PBE[31] and LYP[29] correlation functions, which are among the most popular GGA correlation functionals, with the reLYP correlation functional,[38] which is a new reoptimized version of LYP designed for treating atoms with atomic number greater than 19 (the atoms in the 3d transition series have atomic numbers in the range 21−30), and with the SOGGA11 correlation functional, which is of special interest in this context because it has been shown to be accurate for a wide range of applications in chemistry and physics when combined with the SOGGA11 exchange functional, which shares with C09 an adherence to the correct gradient expansion through second order.

4. THEORY AND METHODS

4.1. Stability Optimization. One important aspect of treating open-shell systems is the symmetry problem. Atoms (and many diatomic molecules) often have higher symmetry than catalytically important complexes with higher metal coordination numbers. However, the goal of this paper is to test the potential abilities of various xc functionals for treating real-world molecules containing transition-metal atoms, and

Table 3. Mean Signed Deviation of 4s Subshell Occupations from that of the Dominant Experimental Configuration in the Stably Optimized SCF Solutions

N12	−0.20	MPWLYP1M	−0.10
OPBE	−0.18	MPWKCIS1K	−0.10
M11-L	−0.17	PBE0	−0.10
LC-ωPBE	−0.17	M06-L	−0.10
M11	−0.17	C09PBE	−0.10
N12-SX	−0.16	B3LYP*	−0.09
BPW91	−0.16	PW86LYP	−0.09
OLYP	−0.16	PW86SOGGA11	−0.09
GVWN3	−0.15	B88	−0.09
OreLYP	−0.15	PW6B95	−0.08
SOGGA	−0.15	ωB97X-D	−0.08
PW91	−0.15	MPW1K	−0.08
HCTH	−0.15	B98	−0.08
BP86	−0.14	M06	−0.08
TPSS	−0.14	B97-2	−0.07
O3LYP	−0.14	CAM-B3LYP	−0.07
PBE	−0.14	ωB97X	−0.07
PW86PBE	−0.14	M05	−0.07
RPBE	−0.14	M08-SO	−0.07
C09LYP	−0.13	B3LYP	−0.07
revTPSS	−0.13	B3V5LYP	−0.07
MOHLYP	−0.13	MPW3LYP	−0.06
SOGGA11	−0.13	M08-HX	−0.05
HSE	−0.12	B97-3	−0.05
τ-HCTH	−0.12	MPW1B95	−0.05
B3PW91	−0.12	SOGGA11-X	−0.05
TPSS1KCIS	−0.12	B1LYP	−0.04
TPSSh	−0.12	B97-1	−0.04
BLYP	−0.12	MPWB1K	−0.04
C09reLYP	−0.11	BHandHLYP	−0.03
LC-MPWLYP	−0.11	M05-2X	−0.01
mPWLYP	−0.11	M06-HF	−0.01
MN12-L	−0.11	BHandH	0.00
PW86reLYP	−0.11	HFPW91	0.00
MN12-SX	−0.11	M06-2X	0.00
C09SOGGA11	−0.11	BMK	0.04
VS98	−0.10	HFLYP	0.05
τ-HCTHhyb	−0.10	HF	0.10

dx.doi.org/10.1021/ct400712k | J. Chem. Theory Comput. XXXX, XXX, XXX−XXX

Table 4. Mean Unsigned Deviation of 4s Subshell Occupation of the Stably Optimized Solution from that of the Dominant Experimental Configuration

HFPW91	0.00	TPSS1KCIS	0.14
M06-2X	0.00	B3PW91	0.14
BHandH	0.00	HSE	0.14
M05-2X	0.02	VS98	0.14
BHandHLYP	0.03	M06-L	0.15
MPWB1K	0.04	MPWLYP1M	0.15
SOGGA11-X	0.05	PW86LYP	0.16
M08-HX	0.05	SOGGA11	0.16
HFLYP	0.05	O3LYP	0.16
M06-HF	0.06	τ-HCTH	0.16
B97-3	0.07	mPWLYP	0.16
B1LYP	0.07	M11	0.17
MPW1B95	0.07	PW86PBE	0.17
B97-1	0.08	BLYP	0.17
MPW1K	0.08	LC-ωPBE	0.17
MPW3LYP	0.08	MOHLYP	0.17
BMK	0.09	C09SOGGA11	0.18
ωB97X	0.09	B88	0.18
PW6B95	0.09	GVWN3	0.18
CAM-B3LYP	0.09	TPSSh	0.18
M05	0.09	PW86reLYP	0.18
M08-SO	0.09	revTPSS	0.18
B3V5LYP	0.10	C09LYP	0.18
B98	0.10	OLYP	0.18
B3LYP	0.10	OreLYP	0.18
ωB97X-D	0.10	HCTH	0.18
M06	0.10	PBE	0.19
MPWKCIS1K	0.10	RPBE	0.19
HF	0.10	SOGGA	0.19
B97-2	0.11	N12-SX	0.19
LC-MPWLYP	0.11	PW91	0.19
PBE0	0.11	BP86	0.19
B3LYP*	0.12	TPSS	0.19
τ-HCTHhyb	0.12	BPW91	0.20
PW86SOGGA11	0.12	OPBE	0.21
C09reLYP	0.12	MN12-L	0.22
MN12-SX	0.12	M11-L	0.22
C09PBE	0.13	N12	0.22

most molecules of interest have low symmetry. Furthermore, it is not theoretically justified to force specific symmetries onto the KS Slater determinant because the KS Hamiltonian need not have the same symmetry as the real electronic Hamiltonian.[3,87,88] As a consequence one needs to consider broken-symmetry solutions, which are solutions to the self-consistent field (SCF) equations that, even in the absence of spin−orbit coupling, do not belong to one of the irreducible representations of the atomic or molecular point group or are not eigenfunctions of $\hat{S}^2$ where $\hat{S}$ is the total electron spin operator.[89,90] For closed-shell systems, which are always singlets, we generally do not find broken-symmetry solutions. However, for systems with a partially filled subshell, such as most cases in this work, the lowest-energy solutions to the KS equations are often found to be broken-symmetry solutions. For these reasons, in all calcuations, we did not require the orbitals or reference Slater determinants to satisfy any symmetry other than having collinear spin−orbitals and having fixed values of M_S. Rather, we chose to obtain the lowest-energy state for each case under consideration by full minimization subject only to the constraint of integer occupation numbers of collinear spin−orbitals with a given M_S.

In order to describe the methods that we used, it is convenient to first define and review some terminology. In all the calculations presented in this article, the spin parts of the spin orbitals are either α or β, i.e., the calculations are collinear. Therefore, M_S, which is the component of total electron spin along the arbitrary spin quantization axis, is a good quantum number and is equal to the half the difference between the number of α electrons and the number of β electrons. The eigenvalues of $\hat{S}^2$ are $S(S+1)$, where S is the total electron spin quantum number; however, the KS Slater determinant need not be an eigenfunction of $\hat{S}^2$. We let n_{SO} be the number of nominally single occupied orbitals (we say "nominally" because [as usual for an unrestricted calculation] the α and β orbitals of a "doubly occupied" pair are not identical.) In all 20 cases (10 atoms, 10 cations) studied in this paper, the ground state has $S = n_{SO}/2$, where n_{SO} is the number of singly occupied orbitals, if any; i.e., the electrons in singly occupied orbitals all have the same spin, which we take as α. In 11 of the cases, the excited state also has $S = n_{SO}/2$. The other nine cases have $S < n_{SO}/2$, which makes them intrinsically multi-determinental and leads to broken-symmetry solutions because KS theory always represents the density by a single Slater determinant. We are interested, for each atom and cation considered, in the lowest excitation that changes the value of S, as enumerated in Table 1.

The SCF optimization of Slater determinants for transition elements is a challenging procedure because the SCF method may not converge to the lowest-energy solution but to some local minimum or just a higher-order extremum (typically a saddle point). This difficulty is exacerbated by the presence of nearly degenerate s and d orbitals in transition metals. In all of our variational calculations we performed a stability analysis[91,92] on the SCF wave functions (by using the "stable = opt" keyword in *Gaussian 09*), followed by reoptimization of the reference wave function if an internal instability was found, and this stabilization procedure was repeated until the lowest-energy solution was obtained with no internal instabilities. In this process all the symmetry constraints were relaxed, as explained above. To verify that we have achieved the global minimum, we recalculated each state of each atom or cation with several different initial guesses and made sure they would converge to an identical solution. The need for stabilization is one of the major complications of using DFT to study open-shell systems, and it will be discussed further in the next subsection.

4.2. Treatment of Open-Shell States. First we classify possible electronic states of a system into one of two categories: nominally single-determinant (NSD) states and intrinsically multideterminant (IMD) states. The NSD states are those with $S = n_{SO}/2$, and the IMD states are those with $S < n_{SO}/2$.

In all cases the energy of NSD states are equated to the stabilized SCF energy of the state with $M_S = S$. It is well-known that the best way to calculate the energy of an IMD state is problematic, and we calculated energies in three ways for all IMD states.

The first method is called the variational method. In this method,

$$E_{IMD}^{var}(n_{SO}, S, M_S) = E_{IMD}^{SCF}(n_{SO}, S, M_S = S) \quad (4)$$

where the right-hand side is the energy of the stably optimized SCF calculation of the state with $M_S = S$.

dx.doi.org/10.1021/ct400712k | J. Chem. Theory Comput. XXXX, XXX, XXX−XXX

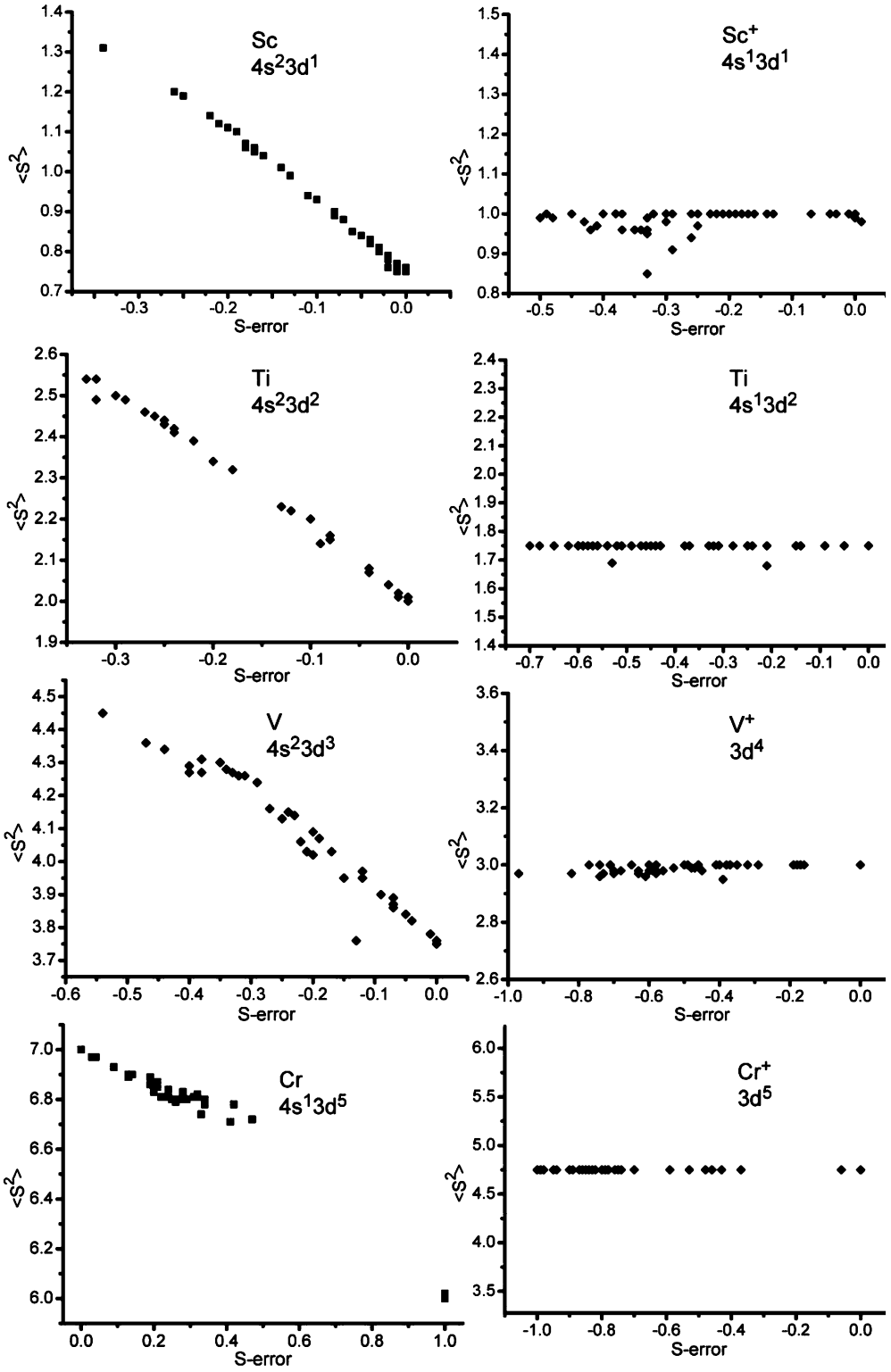

Figure 1. Plots of $\langle S^2 \rangle$ values versus s-orbital-occupancy error for M and M^+ (M = Sc, Ti, V, Cr).

However, when one optimizes a state with $M_S = S < n_{SO}/2$, it is always possible to form, from the same orbitals as those in the optimized state, another $M_S = S$ state that has $S = n_{SO}/2$. Because our xc functionals are not exact, the optimized state can be considered to be a mixture of these two states; this situation is often signaled by the $\langle S^2 \rangle$ value of the SCF solution.[93] For example, in the simplest case of an open-shell singlet which has two unpaired electrons, one of α spin and one of β spin, one sometimes finds $\langle S^2 \rangle = 1.0$. If the spatial parts of the spin orbitals were the same in the singlet and the triplet, such a broken-symmetry solution could be considered to be a 50:50 mixture of the corresponding singlet ($\langle S^2 \rangle = 0$) and triplet ($\langle S^2 \rangle = 2$) states, and the energy difference between the real singlet and the triplet would reasonably be approximated as twice the energy difference between the calculated broken-symmetry $M_S = 0$ state and the triplet $M_S = 1$ state. The

dx.doi.org/10.1021/ct400712k | J. Chem. Theory Comput. XXXX, XXX, XXX−XXX

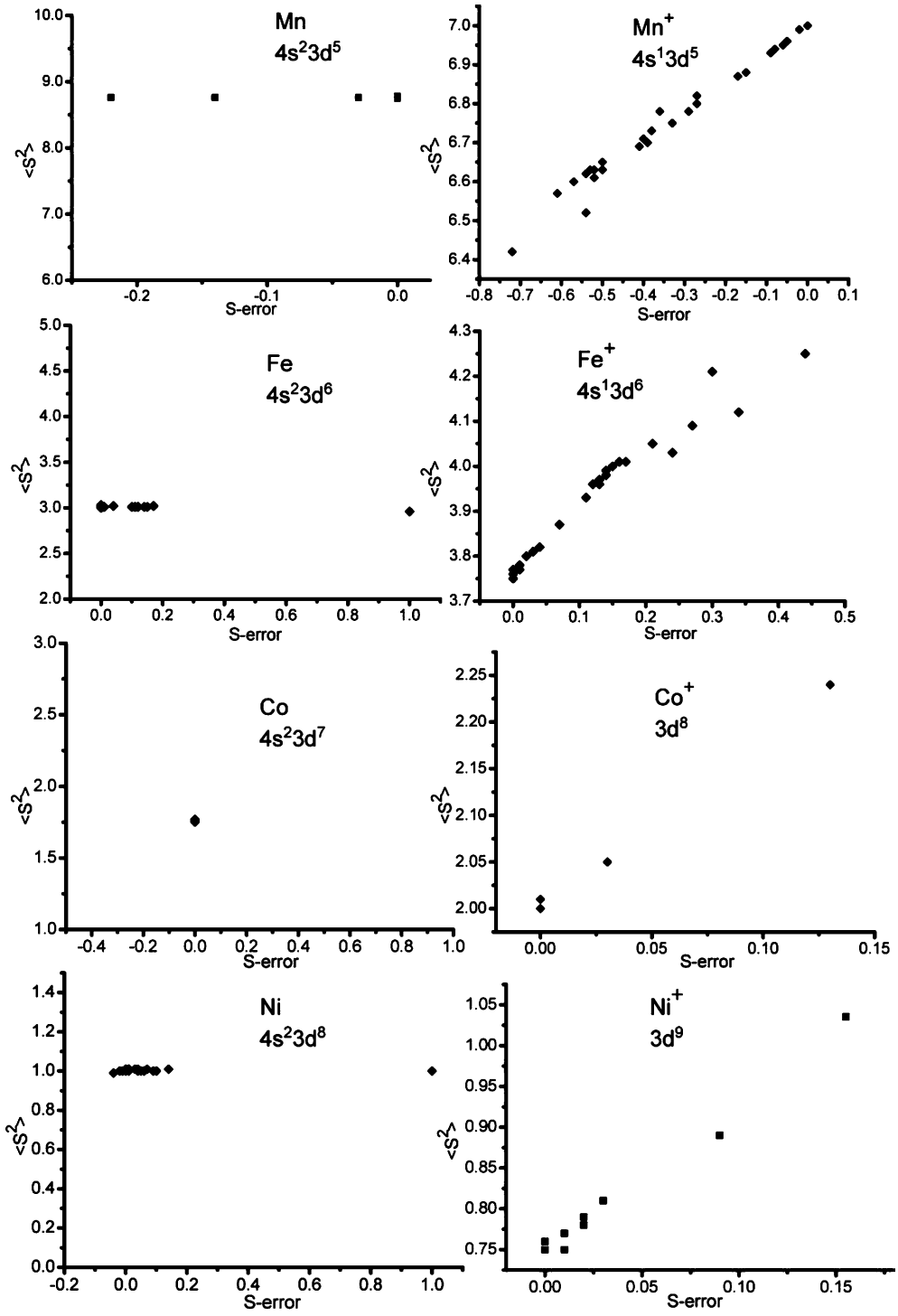

Figure 2. Plots of $<S^2>$ values versus s-orbital-occupancy error for M and M^+ (M = Mn, Fe, Co, Ni).

generalization of this situation to other multiplicities has been called the weighted-average broken symmetry (WABS) method, and it is our second method. The result is encapsulated in the formula given by Yamaguchi,[94] which yields

$$E_{\mathrm{IMD}}^{\mathrm{WABS}}(n_{\mathrm{SO}}, S, M_{\mathrm{S}}) = E_{\mathrm{NSD}}^{\mathrm{SCF}}(n_{\mathrm{SO}}, S = n_{\mathrm{SO}}/2, M_{\mathrm{S}} = n_{\mathrm{SO}}/2) - k[E_{\mathrm{NSD}}^{\mathrm{SCF}}(n_{\mathrm{SO}}, S = n_{\mathrm{SO}}/2, M_{\mathrm{S}} = n_{\mathrm{SO}}/2) - E_{\mathrm{IMD}}^{\mathrm{SCF}}(n_{\mathrm{SO}}, S, M_{\mathrm{S}} = S)] \quad (5)$$

where

$$k = n_{\mathrm{SO}}/[\,<S^2>_{\mathrm{NSD}}^{\mathrm{SCF}}(n_{\mathrm{SO}}, S = n_{\mathrm{SO}}/2, M_{\mathrm{S}} = n_{\mathrm{SO}}/2) - <S^2>_{\mathrm{IMD}}^{\mathrm{SCF}}(n_{\mathrm{SO}}, S, M_{\mathrm{S}} = S)] = \frac{2S_{\mathrm{HS}}}{<S^2>_{\mathrm{HS}} - <S^2>_{\mathrm{BS}}} \quad (6)$$

This method has become popular in practical applications and has been discussed in detail elsewhere.[4,87]

A theoretical objection to this second approach is that eqs 5 and 6 are derived under the assumption that the IMD and NSD

dx.doi.org/10.1021/ct400712k | J. Chem. Theory Comput. XXXX, XXX, XXX−XXX

states have the same spatial orbitals such that the only difference between these states is that in the NSD state all singly occupied orbitals are α orbitals, while in the IMD state one or more of these orbitals become occupied by a β electron. Nevertheless the Yamaguchi formula is popularly applied even if one is uncertain regarding the validity of these assumptions, merely with knowledge of their energies and $<S^2>$ values. Hence it is important to test this formula, and in our second method we utilized Yamaguchi formula for all IMD cases, even when orbitals that are occupied in the NSD state do not correspond to those that are occupied in the IMD state.

In our third method, for each IMD state, we calculated the SCF energy of an artificial $S = n_{SO}/2$ state with the same orbitals as in the IMD state (we obtain this state by flipping the spin of one or more singly occupied orbital), and this post-SCF state (labeled PSCF in equations) was used for the $S = n_{SO}/2$ state in eq 5, with the true IMD state still used in eqs 7 and 8. We call this the reinterpreted broken symmetry (RBS) approach. This yields

$$E^{RBS}_{IMD}(n_{SO}, S, M_S) = E^{PSCF}(n_{SO}, S = n_{SO}/2, M_S = n_{SO}/2) - k[E^{PSCF}(n_{SO}, S = n_{SO}/2, M_S = n_{SO}/2) - E^{SCF}_{IMD}(n_{SO}, S, M_S = S)] \quad (7)$$

where

$$k = n_{SO}/[< S^2 >^{PSCF} (n_{SO}, S = n_{SO}/2, M_S = n_{SO}/2) - <S^2 >^{SCF}_{IMD} (n_{SO}, S, M_S = S)] = \frac{2S_{HS}}{<S^2>_{HS} - <S^2>_{BS}} \quad (8)$$

For example, consider the state Fe(^{3}F, 4s^{1}3d^7). In the variational method, the energy difference between ^{3}F and ^{5}D SCF states was calculated from the two stabilized SCF calculations. In the WABS method, the triplet state was calculated by the Yamaguchi formula where the NSD state is the stabilized quintet state, which is the Fe(^{5}D, 4s^{2}3d^6) state. For the RBS method, we need to consider the nature of the triplet state; it turns out that, for all the xc functionals under test in the present article, the triplet state has three dα electrons and one sβ electron. We therefore calculate a post-SCF artificial quintet state by flipping the spin of the s electron, and we obtain the energy of the triplet using eqs 7 and 8 with this artificial post-SCF quintet state, which is nominally a state with 4s^{1}3d^7. If the triplet had been a state with two dα electrons, one dβ electron, and one sα electron, we would have had to flip the dβ electron.

The most appropriate way to flip the 4s β electron would take exactly the same β orbital and occupy it with an α electron. Since the spatial part of α and β orbitals are generally not orthogonal to each other, this step would require additional orthogonalization. To alleviate the computational complications, we flip the electron by identifying the α virtual orbital that is most similar to the β orbital we intend to flip and calculate the post-SCF NSD state energy by occupying this particular α orbital. This works well when the orbitals of both spins are similar to each other, which is usually true. However, for some atoms, some of the density functionals produce states where the highest-energy nominally doubly occupied orbitals are very different for the α and β electrons. The RBS method is inappropriate for these cases and can produce very large errors. We recommend that when the flipped-state post-SCF energy is higher than the unflipped-state energy by more than 100 kcal/mol, one should apply neither the WABS method nor the RBS method. The cases where one of more functionals raise the energy of the flipped state by more than 100 kcal/mol are the singlet state of Ni and doublet state of Co. If we delete excitation energies and ionization potentials that involve these states, there are only 28 of the 30 data available, and—among other statistical measures—we will give mean-unsigned errors (MUEs) for these 28 cases to provide a more useful estimate of which functionals prove most accurate if a user restricts using the WABS and RBS method to cases where these methods are recommended.

4.3. Orbital Analysis. According to experimental data, there are nine cases of species with IMD electronic configurations, namely Sc$^+$(^{1}D, 4s^{1}3d^1), Ti$^+$(^{2}F, 4s^{1}3d^2), V$^+$(^{3}F, 4s^{1}3d^3), Cr(^{5}S, 4s^{1}3d^5), Cr$^+$(^{4}D, 4s^{1}3d^4), Mn$^+$(^{5}S, 4s^{1}3d^5), Fe(^{3}F, 4s^{1}3d^7), Co(^{2}F, 4s^{1}3d^8), and Ni(^{1}D, 4s^{1}3d^9). In four of these cases, Sc$^+$(^{1}D, 4s^{1}3d^1), Ti$^+$(^{2}F, 4s^{1}3d^2), Cr(^{5}S, 4s^{1}3d^5), and Mn$^+$(^{5}S, 4s^{1}3d^5), the correct corresponding NSD state is the ground state, and the only difference between the NSD and post-SCF states is that for the post-SCF ones, the orbitals are not optimized but rather are taken to be the same as in the IMD state. In the other five cases, V$^+$(^{3}F, 4s^{1}3d^3), Cr$^+$(^{4}D, 4s^{1}3d^4), Fe(^{3}F, 4s^{1}3d^7), Co(^{2}F, 4s^{1}3d^8), and Ni(^{1}D, 4s^{1}3d^9), the post-SCF state used for eqs 7 and 8 has different orbitals occupied than the ground states. This is clear for atoms where the orbitals have distinct symmetries, but it would not always be obvious for low-symmetry molecules, e.g., in C_1 symmetry where all the orbitals have the same symmetry.

The analysis is complicated by the fact that the calculated electronic states do not always correspond to the experimental ones. In many cases the calculated orbitals are described as spatial-symmetry-broken combinations of s and d orbitals, and the electronic configuration consequently has fractional atomic-orbital occupancy. The discrepancy between the experimental and calculated number of s electrons (s occupancy error) is given in Tables 3 and 4 (note that p orbitals do not participate in this mixing because they have different symmetry with regards to the inversion center).

We analyzed the correlation between s-orbital-occupancy error and spin-contamination of the Slater determinant, and we found two kinds of cases.

In the first kind of case $<S^2>$ depends on s-orbital-occupancy error linearly. Cases of this type are Sc(^{2}D, 4s^{2}3d^1), Ti(^{3}F, 4s^{2}3d^2), V(^{4}F, 4s^{2}3d^3), Cr(^{5}S, 4s^{1}3d^5), Mn$^+$(^{5}S, 4s^{1}3d^5), Fe$^+$(^{4}F, 3d^7), Co$^+$(^{3}F, 3d^8), and Ni$^+$(^{2}D, 3d^9). For electronic states of this type, the shift of electron density from an s orbital to d orbitals results in a state that is a mixture of two states: multideterminant and single-determinant. For example, for Sc(^{2}D, 4s^{2}3d^1) some functionals give a state where a β s-electron is partially moved to a d orbital, which means that the resulting state is a mixture of the experimentally observed nominally single-determinant state Sc(^{2}D, 4s^{2}3d^1) and a multideterminant state Sc(4s^{1}3d^2) with electrons with opposite spins occupying two different d orbitals. The interesting opposite situation is observed for Cr(^{5}S, 4s^{1}3d^5). The initial state is multideterminantal, while a shift of the β s-electron to any of five singly occupied d orbitals results in mixture of the experimental state and a single-determinant Cr(3d^6) state.

The second type of case includes Sc$^+$(^{1}D, 4s^{1}3d^1), Ti$^+$(^{2}F, 4s^{1}3d^2), V$^+$(^{3}F, 4s^{1}3d^3), Cr$^+$(^{4}D, 4s^{1}3d^4), Mn(^{6}S, 4s^{2}3d^5), Fe(^{3}F, 4s^{1}3d^7), Co(^{2}F, 4s^{1}3d^8), and Ni(^{1}D, 4s^{1}3d^9), where $<S^2>$

dx.doi.org/10.1021/ct400712k | J. Chem. Theory Comput. XXXX, XXX, XXX−XXX

Table 5. MSE(9) and MUE(9) of ΔE(s → d excitation) for the Variational Method

functional	MSE (kcal/mol)	MUE (kcal/mol)	functional	MSE (kcal/mol)	MUE (kcal/mol)
SOGGA11-X	−2.0	2.7	OreLYP	1.9	9.5
M08-HX	0.1	3.2	RPBE	−3.2	9.9
M08-SO	−0.1	4.4	SOGGA11	−1.7	9.9
M06	2.8	4.5	BP86	−3.0	9.9
B97-3	0.2	4.5	MPWKCIS1K	−6.1	10.0
B97-1	2.2	5.3	PW86PBE	−4.2	10.2
M06-2X	0.0	5.3	PBE0	−6.6	10.2
B98	1.8	5.4	PBE	−3.8	10.2
ωB97X-D	0.6	5.4	MPW1K	−9.2	10.3
M06-L	−1.0	5.5	HCTH	7.3	10.5
ωB97X	5.4	5.7	PW91	−3.7	10.5
PW86reLYP	−0.6	6.1	SOGGA	−4.6	10.6
CAM-B3LYP	−1.6	6.6	B3PW91	−5.8	10.7
PW86LYP	−1.1	6.7	revTPSS	−4.7	10.7
MPWB1K	−6.0	6.9	TPSS	−4.0	10.8
B97-2	4.3	7.2	TPSS1KCIS	−4.0	10.9
PW6B95	−3.3	7.3	TPSSh	−4.7	11.0
C09reLYP	−0.8	7.3	BPW91	−5.0	11.0
B1LYP	−3.9	7.3	C09PBE	−5.8	11.1
MPW3LYP	−2.8	7.3	LC-ωPBE	−0.5	11.2
MPW1B95	−4.2	7.3	HSE	−6.7	11.2
BHandH	−7.7	7.7	OLYP	1.1	11.3
BMK	−5.2	7.7	C09SOGGA11	−7.3	11.8
B3V5LYP	−3.1	7.9	M11	0.6	11.8
M05-2X	1.9	7.9	PW86SOGGA11	−2.6	12.3
B3LYP	−2.9	7.9	N12-SX	9.3	12.6
VS98	−0.5	8.0	M06-HF	0.4	12.9
τHCTHhyb	5.3	8.2	GVWN3	−0.5	13.0
B3LYP*	−2.2	8.2	MN12-L	11.1	13.4
BHandHLYP	−7.3	8.3	OPBE	−2.3	13.5
LC-MPWLYP	3.4	8.3	B88	−13.3	15.8
M05	8.1	8.4	τHCTH	15.9	16.6
MPWLYP1M	−0.8	8.5	HFPW91	−16.4	17.0
MOHLYP	0.0	8.6	M11-L	4.8	17.3
mPWLYP	−0.4	8.8	MN12-SX	18.2	18.2
BLYP	−1.0	9.2	HFLYP	−14.0	20.1
C09LYP	−1.8	9.2	N12	3.5	20.8
O3LYP	−0.4	9.3	HF	−27.2	28.0

does not depend on s-orbital-occupancy error. Here both GS and ES states are multideterminantal, except for the single-determinant Mn(^{6}S, $4s^2 3d^5$). For Fe(^{3}F, $4s^1 3d^7$), Co(^{2}F, $4s^1 3d^8$), and Ni(^{1}D, $4s^1 3d^9$) the situation is much simpler because in all of these three cases the electron configuration has either exactly integer occupations or one that is very close to an integer (see Table 1). In all these three cases the stably optimized ground states do not have the same orbitals occupied as the excited states, so the post-SCF states Fe(quintet $4s^1 3d^7$), Co(quartet $4s^1 3d^8$), and Ni(triplet $4s^1 3d^9$), are quite different from the stably optimized states.

Figures 1 and 2 illustrate the above observations by presenting plots of $\langle S^2 \rangle$ versus s-occupancy error.

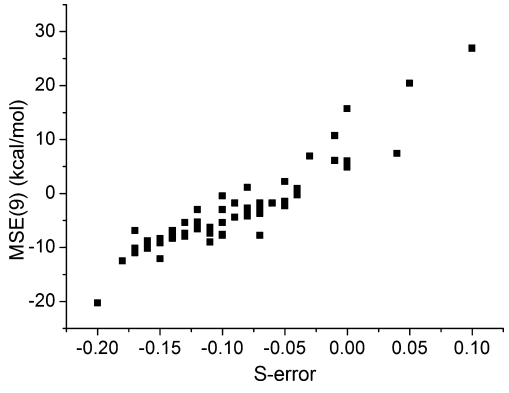

Figure 3. Correlation between s-orbital-occupancy error (Table 3) and MSE(9) (Table 12).

5. RESULTS

5.1. Orbital Bias: s and d Orbitals. Let us first consider the s-orbital-occupancy error of various xc functionals because this is one possible criterion for assessing each functional's ability to describe the s and d orbitals in a balanced manner. Table 3 shows that DFT functionals with a small percentage X of Hartree−Fock exchange tend to have negative s-orbital-occupancy error, while functionals with high Hartree−Fock exchange tend to have less negative or even slightly positive s-orbital-occupancy error, and the predicted electronic configuration is closer to the experimental dominant configuration, as

dx.doi.org/10.1021/ct400712k | J. Chem. Theory Comput. XXXX, XXX, XXX−XXX

Table 6. MSE(9) and MUE(9) of ΔE(s → d excitation) for WABS Method

functional	MSE (kcal/mol)	MUE (kcal/mol)	functional	MSE (kcal/mol)	MUE (kcal/mol)
B97-3	−1.6	3.2	PBE0	−8.3	8.5
B97-1	0.6	3.7	M05	6.6	8.6
B98	0.1	3.7	PW86PBE	−5.6	8.8
ωB97X-D	−1.1	3.8	PBE	−5.2	8.8
ωB97X	3.7	4.0	revTPSS	−6.0	9.0
M08-HX	−2.2	4.7	PW91	−5.1	9.1
M06	0.9	5.0	TPSS	−5.3	9.2
CAM-B3LYP	−3.1	5.1	SOGGA	−6.3	9.2
SOGGA11-X	−4.7	5.4	B3PW91	−7.1	9.3
PW6B95	−4.9	5.6	BMK	−7.8	9.4
B97-2	2.8	5.6	TPSSh	−6.0	9.5
MPW3LYP	−4.4	5.7	TPSS1KCIS	−5.2	9.5
C09reLYP	−2.3	5.7	MPWKCIS1K	−7.6	9.6
B1LYP	−5.6	6.0	C09PBE	−7.6	9.6
MPW1B95	−6.0	6.0	BPW91	−6.5	9.6
M06-L	−2.4	6.0	OLYP	0.0	9.7
B3V5LYP	−4.6	6.3	HSE	−8.1	9.8
B3LYP	−4.3	6.4	LC-ωPBE	−1.6	10.2
M08-SO	−2.7	6.5	BHandH	−10.4	10.4
VS98	−2.2	6.7	BHandHLYP	−10.0	10.8
πHCTHhyb	4.0	6.7	M11	−0.4	10.8
B3LYP*	−3.5	6.8	M05-2X	−1.4	11.2
PW86reLYP	−2.8	7.0	MPW1K	−11.4	11.4
MOHLYP	−1.0	7.0	PW86SOGGA11	−3.3	11.6
PW86LYP	−2.8	7.0	GVWN3	−1.9	11.8
MPWLYP1M	−2.0	7.1	N12-SX	8.9	12.1
M06-2X	−2.4	7.3	OPBE	−4.0	12.2
LC-MPWLYP	2.4	7.3	C09SOGGA11	−9.7	12.7
mPWLYP	−1.4	7.4	M06-HF	−0.8	14.0
BLYP	−2.1	7.8	MN12-L	9.7	14.5
C09LYP	−3.1	7.8	B88	−15.4	15.4
OreLYP	0.7	7.8	πHCTH	15.5	15.6
O3LYP	−1.5	7.9	M11L	4.4	16.0
MPWB1K	−8.2	8.2	MN12SX	16.6	17.6
HCTH	6.6	8.3	N12	2.6	20.2
RPBE	−4.5	8.4	HFPW91	−20.5	21.0
SOGGA11	−3.0	8.4	HFLYP	−18.3	24.4
BP86	−4.4	8.5	HF	−32.1	32.9

can be seen also from the MUEs in Table 4. This is consistent with other studies.[6,95]

An obvious implication from this observation is that a judicious percentage of Hartree−Fock exchange is necessary for obtaining a balanced treatment of s and d electrons, which is further verified by considering excitation energies with s → d transitions. According to the experimental data, in the 20 multiplicity-changing transitions under consideration, 12 cases involve electron excitations between s and d orbitals. These cases are Sc, Ti, V, V^+, Cr^+, Fe, Fe^+, Co, Co^+, Ni, Ni^+, and Cu^+. The average difference (over 76 methods) between number of s electrons for IMD and NSD states are 0.9, 0.9, 0.8, 0.3, 0.3, 0.7, 0.9, 0.7, 1.0, 0.4, 1.0, and 1.0 for each case respectively. Due to s-orbital-occupancy error, in the cases of V^+, Cr^+, and Ni, many functionals incorrectly predict the electronic state, resulting in both states presenting about the same number of s and d electrons, so they are excluded from further discussions of this aspect, and we only considered the nine remaining cases. Tables 5−7 show the performance of various functionals for prediction of s → d excitation of the nine species above. It is interesting to compare data from Tables 3 and 7, because they both are related to the calculated energy gaps between s and d orbitals. The scattergram obtained this way is presented in Figure 3, which clearly shows that methods with negative s-orbital-occupancy error tend to underestimate energy of s → d excitation and vice versa. This makes perfect sense since a negative s-orbital-occupancy error implies a bias of the corresponding functional toward the d orbitals, which leads to a smaller s → d transition energy and vice versa.

Table 6 allows us to put the overstabilization of d orbitals relative to s orbitals by Hartree−Fock exchange on a quantitative basis. For example, HFLYP has an MSE for s → d excitation energies of −18.3 kcal/mol, whereas mPWLYP, BLYP, and OLYP, which have precisely the same correlation functional but local exchange, have MSEs of −1.4, −2.1, and −0.0 kcal/mol, respectively. B1LYP, which is 20:80 mixture of HFLYP and BLYP, has an MSE of 0.7 kcal/mol, much closer to the value for BLYP than to that for HFLYP. Correlation favors s orbitals, as seen by comparing the MSEs for HF (−32.1 kcal/mol) and HFLYP (−18.3 kcal/mol) or B88 (−15.4 kcal/mol) and BLYP (−2.1 kcal/mol); the differences are remarkably similar (13.8 and 13.6 kcal/mol). Similarly Table 6 shows that

dx.doi.org/10.1021/ct400712k | J. Chem. Theory Comput. XXXX, XXX, XXX−XXX

Table 7. MSE(9) and MUE(9) of ΔE(s → d excitation) for RBS Method

functional	MSE (kcal/mol)	MUE (kcal/mol)	functional	MSE (kcal/mol)	MUE (kcal/mol)
SOGGA11-X	−2.1	2.8	PBE	−3.0	8.2
M06-L	0.8	4.2	PW91	−2.9	8.3
M06	3.1	4.3	BHandHLYP	−7.5	8.3
B97-3	0.1	4.3	SOGGA	−3.7	8.4
M08-SO	1.6	4.6	TPSS	−3.5	8.4
M08-HX	1.9	5.0	revTPSS	−4.4	8.6
B98	1.6	5.0	BPW91	−4.0	8.7
ωB97X-D	0.2	5.1	OLYP	3.1	8.8
B971	2.0	5.1	PW86PBE	−5.6	8.8
C09reLYP	−2.3	5.7	LC-MPWLYP	4.3	9.0
ωB97X	5.5	5.8	M05	8.8	9.1
CAM-B3LYP	−1.8	6.3	PBE0	−7.3	9.2
M06-2X	1.4	6.5	TPSS1KCIS	−4.2	9.4
PW6B95	−3.8	6.6	TPSSh	−5.0	9.4
MPWB1K	−6.4	6.7	B3PW91	−6.4	9.5
MPW1B95	−4.8	6.7	C09PBE	−7.6	9.6
B1LYP	−4.4	6.7	MPW1K	−9.8	9.9
MPW3LYP	−3.3	6.7	HSE	−7.4	10.2
MOHLYP	2.1	6.7	OPBE	−0.1	10.2
B97-2	4.4	6.9	MPWKCIS1K	−9.4	10.2
PW86reLYP	−2.8	7.0	SOGGA11	2.1	10.2
PW86LYP	−2.8	7.0	HCTH	10.2	10.5
B3V5LYP	−3.5	7.1	LC-ωPBE	−0.1	10.9
B3LYP	−3.3	7.2	GVWN3	0.0	11.1
M05-2X	2.5	7.3	B88	−11.1	11.5
OreLYP	2.9	7.4	PW86SOGGA11	−3.3	11.6
B3LYP*	−2.5	7.4	N12-SX	9.3	12.6
MPWLYP1M	−0.6	7.5	C09SOGGA11	−9.7	12.7
mPWLYP	0.4	7.5	MN12-L	11.2	14.2
BMK	−5.9	7.6	M06-HF	4.1	15.4
RPBE	−1.9	7.6	M11-L	5.4	15.8
BLYP	−0.3	7.7	M11	4.7	15.8
BP86	−2.1	7.8	HFPW91	−15.9	16.4
C09LYP	−3.1	7.8	πHCTH	18.9	18.9
VS98	0.3	7.9	HFLYP	−13.0	19.1
BHandH	−7.9	7.9	HF	−26.1	26.9
O3LYP	0.1	8.0	N12	11.2	27.2
HCTHhyb	5.5	8.1	MN12-SX	29.0	29.0

PW91 correlation overly favors s orbitals by a sightly smaller amount than LYP, in particular comparing HFPW91 to HF shows a difference of 11.6 kcal/mol (which may fairly be compared to the 13.8 kcal/mol difference mentioned in the previous sentence). This is very relevant because PW91 correlation is almost the same as the widely used PBE correlation.

Some functionals have MSEs of absolute magnitude <2 kcal/mol in Table 6, namely B97-3, B97-1, B98, ωB97X-D, M06, MOHLYP, MPWLYP1M, mPWLYP, OreLYP, O3LYP, OLYP, LC-ωPBE, M11, M05-2X, GVWN3, with X values of 26.93, 21, 21.98, 22.2−100.0, 27, 0, 5, 0, 0, 11.61, 0, 0−100, 42.8−100, 56, and 0, respectively. Many other functionals with X in this range do worse or even much worse, so clearly the systematic errors depends on much more than the just the value of X.

In Table 7, SOGGA11-X and M06 have MSEs with magnitudes larger than 2.0 kcal/mol, but—along with M06-L and B97-3—are among the four leading MUEs in Table 7.

5.2. Spin States and Ionization Potentials. Next we turn to the errors for energies of excitation from ground states to excited states, calculated by the variational, WABS, and RBS methods, as given in Tables 8−10, respectively. In all three tables the methods are sorted according their mean-unsigned error, MUE(20), for the 20 cases. We find the accuracy of RBS to be almost equal to that of the WABS, and thus it is potentially another choice for treating the broken-symmetry problem; we prefer RBS because it uses only the orbitals optimized for the IMD state to calculate its energy, which seems more consistent with the assumptions of the Yamaguchi formula. It is also clear that the variational method is the worst among the three methods, implying that either RBS or WABS should be used as long as the system does not conflict the general criteria for application of them. According to the RBS results in Table 10, one concludes that the six best functionals for excitation energies are SOGGA11-X, ωB97X-D, MPW1B95, MPW1K, B97-3, and CAM-B3LYP.

Table 10 shows that the MUE of B3LYP*, which is a functional specifically reparametrized for spin states of 3d-series transition-metal compounds, is 5.8 kcal/mol, somewhat worse than that of the older B3LYP method (5.3 kcal/mol).

The errors for ionization potentials for the variational, the WABS, and the RBS methods are given in Tables 11−13.

dx.doi.org/10.1021/ct400712k | J. Chem. Theory Comput. XXXX, XXX, XXX−XXX

Table 8. MSE(20) and MUE(20) of ΔE (kcal/mol) for the Variational Method

functional	MSE	MUE	functional	MSE	MUE
SOGGA11-X	0.7	3.8	C09reLYP	4.3	8.0
M08-SO	2.0	4.4	PW91	0.5	8.0
MPW1B95	−0.8	4.6	B97-2	6.7	8.1
MPWB1K	−2.4	5.1	VS98	3.3	8.1
M08-HX	2.3	5.1	MPW1K	−6.3	8.1
PW6B95	0.4	5.1	BPW91	−0.8	8.2
wB97X-D	3.1	5.3	SOGGA	−1.0	8.3
B97-3	3.8	5.8	BHandHLYP	−2.2	8.5
CAM-B3LYP	2.1	5.9	MPWLYP1M	4.3	8.5
B1LYP	1.1	6.1	SOGGA11	2.1	8.6
B3V5LYP	1.6	6.5	C09PBE	−2.4	8.7
MPW3LYP	2.0	6.5	M11	0.3	8.7
B98	4.9	6.5	BLYP	4.3	8.9
B3LYP	1.8	6.6	C09SOGGA11	−3.2	9.0
MPWKCIS1K	−2.9	6.7	PW86LYP	5.6	9.0
PBE0	−3.3	6.7	PW86SOGGA11	1.2	9.1
BHandH	−2.5	6.8	mPWLYP	5.0	9.1
B97-1	5.4	6.8	πHCTHhyb	7.8	9.2
M06-L	2.9	6.8	OLYP	4.7	9.3
B3PW91	−2.5	6.9	OreLYP	6.0	9.4
TPSSh	−1.5	7.0	PW86reLYP	6.7	10.0
B3LYP*	2.4	7.0	OPBE	−0.4	10.1
revTPSS	−0.9	7.1	M06-2X	6.8	10.2
TPSS1KCIS	−0.9	7.1	M05-2X	7.2	10.5
LC-MPWLYP	5.0	7.2	GVWN3	3.3	10.6
HSE	−3.3	7.3	M05	10.8	11.3
RPBE	0.7	7.3	B88	−9.0	11.7
O3LYP	3.0	7.4	N12-SX	10.0	11.7
TPSS	−0.2	7.5	HCTH	10.4	11.9
ωB97X	7.4	7.5	MN12-L	10.9	12.0
LC-ωPBE	−0.2	7.6	M11-L	4.2	14.1
BMK	0.1	7.6	N12	6.7	15.9
M06	6.3	7.7	HFPW91	−13.0	16.5
PBE	0.3	7.7	πHCTH	16.6	16.9
MOHLYP	3.9	7.8	MN12-SX	18.6	18.7
PW86PBE	0.5	7.8	HFLYP	−7.8	19.4
BP86	1.5	7.9	M06-HF	9.8	21.4
C09LYP	2.9	7.9	HF	−20.4	24.0

Table 9. MSE(20) and MUE(20) of ΔE (kcal/mol) for WABS Method

functional	MSE	MUE	functional	MSE	MUE
B97-3	1.3	4.0	M11	−1.9	7.7
ωB97X-D	0.3	4.2	LC-ωPBE	−2.9	7.7
PW6B95	−2.4	4.2	PBE	−2.5	7.8
CAM-B3LYP	−0.5	4.3	PW86PBE	−2.1	7.8
MPW1B95	−3.7	4.3	PW91	−2.3	7.9
B1LYP	−1.5	4.4	πHCTHhyb	5.4	8.2
MPW3LYP	−0.5	4.7	M06	3.3	8.2
M08-HX	−0.3	4.7	PW86SOGGA11	−0.8	8.2
B3V5LYP	−0.9	4.8	OLYP	2.4	8.2
M08-SO	−1.0	4.9	OreLYP	3.6	8.2
B3LYP	−0.7	4.9	BMK	−3.3	8.2
B98	2.4	5.0	BPW91	−3.7	8.4
B97-1	2.9	5.2	PW86LYP	3.1	8.5
B3LYP*	−0.1	5.6	SOGGA	−4.1	8.6
MPWB1K	−5.7	5.7	SOGGA11	−0.7	8.8
SOGGA11-X	−3.2	5.9	VS98	−0.1	8.8
LC-MPWLYP	2.8	5.9	C09PBE	−5.6	9.0
ωB97X	4.9	6.0	BHandHLYP	−5.6	9.1
O3LYP	0.6	6.2	PW86reLYP	4.1	9.6
MOHLYP	1.7	6.5	C09SOGGA11	−6.4	9.9
RPBE	−1.9	6.8	MPW1K	−10.1	10.1
PBE0	−6.4	6.8	OPBE	−3.5	10.2
revTPSS	−3.5	6.8	GVWN3	0.4	10.6
TPSSh	−4.1	6.9	M06-2X	5.2	10.9
MPWKCIS1K	−5.8	6.9	N12-SX	8.7	11.0
TPSS1KCIS	−3.5	6.9	HCTH	8.6	11.0
C09reLYP	1.8	6.9	M05	8.4	11.4
TPSS	−2.8	7.0	MN12-L	9.1	11.8
MPWLYP1M	2.1	7.0	M05-2X	4.3	11.8
B97-2	4.1	7.1	B88	−12.6	13.0
B3PW91	−5.4	7.1	M11-L	2.1	14.2
C09LYP	0.5	7.2	N12	4.2	16.2
BHandH	−6.0	7.2	πHCTH	15.0	16.5
M06-L	0.0	7.2	MN12-SX	17.3	18.7
BP86	−1.0	7.3	HFPW91	−18.2	18.9
HSE	−6.3	7.4	HFLYP	−12.5	22.4
BLYP	2.1	7.5	M06-HF	10.6	23.3
mPWLYP	2.8	7.7	HF	−25.6	27.4

Although most of the ground states of both atoms and cations are NSD states, the spin-contamination from an unbalanced treatment of s and d orbitals in many states still leads to a slightly different corrected energy with WABS or RBS method. Thus for more than half of the xc functionals under examination, we find changes in MSE as well as MUE values across Tables 11−13, further resulting in variations in performance rankings. An immediate observation is the good performance of the B97-X (X = 1−3) series of functionals, all with an MUE(10) of <4.0 kcal/mol in all three tables. Other best methods in Table 12 are B98, ωB97X-D, PW6B95, ωB97X, B1LYP, M08-SO, MPW1B95, and CAM-B3LYP, all of which have an MUE(10) < 4.0 kcal/mol. Most of them perform well also for excitation energies using the RBS correction. However, SOGGA11-X, which is one of the best methods for excitation energies, has a larger error of 6.8 kcal/mol.

The overall performance for excitation energies and ionization potentials, calculated as the MUE(30), is given in Table 14, where the methods are sorted according to their performance for IP and excitation energies with RBS corrections. Although the RBS method attempts to account for variation in orbital character better than the WABS method, this orbital variation can still be a source of problems, as already discussed briefly in Section 4.2. When a low-spin state has an orbital flipped, we remove one electron from a minority-spin orbital (i.e., a β orbital) and place in the majority-spin (i.e., α) manifold. Sometimes the orbital one wants to flip is not the highest-energy β orbital, and we were careful to find the right orbital in every case by a manual search. However, there is another problem that is harder to handle, namely that some combinations of functional and atomic state produce very different α and β orbitals. For example, singlet Ni is an open-shell singlet with one α electron in 3d and one β electron in 4s, and the eight other valence electrons paired in the remaining four 3d orbitals. However, some functionals, such as M06-HF and MN12-SX, produce very different orbitals for α and β electrons; in these cases the β-HOMO is not a pure 4s orbital but has a strong mixing of 3d orbitals, while the α-LUMO is a very "pure" 4s orbital. When the β-HOMO is moved to the α manifold, the resulting post-SCF high-spin state is very high in

dx.doi.org/10.1021/ct400712k | J. Chem. Theory Comput. XXXX, XXX, XXX−XXX

Table 10. MSE(20) and MUE(20) of ΔE (kcal/mol) for RBS Method

functional	MSE	MUE	functional	MSE	MUE
SOGGA11-X	0.1	3.6	HSE	−4.5	7.7
ωB97X-D	1.9	4.3	M08-HX	5.0	7.8
MPW1B95	−2.6	4.5	PW86PBE	−2.1	7.8
MPWB1K	−3.8	4.5	SOGGA	−1.8	7.9
B97-3	3.0	4.9	OLYP	5.1	8.0
CAM-B3LYP	1.3	5.1	VS98	2.6	8.0
B3V5LYP	0.3	5.2	mPWLYP	4.7	8.1
B3LYP	0.4	5.3	PW86SOGGA11	−0.8	8.2
B98	3.9	5.5	MPW1K	−7.8	8.4
PW6B95	−0.1	5.5	πHCTHhyb	7.2	8.5
M08-SO	3.9	5.6	BHandHLYP	−2.1	8.5
MPW3LYP	1.0	5.6	PW86LYP	3.1	8.5
B97-1	4.4	5.8	MPWKCIS1K	−7.7	8.5
BHandH	−3.5	5.8	OPBE	−0.4	8.7
B3LYP*	1.1	5.8	OreLYP	6.5	8.7
B1LYP	0.7	5.9	LC-ωPBE	0.3	8.8
revTPSS	−1.5	6.0	SOGGA11	3.4	8.8
RPBE	0.5	6.0	C09PBE	−5.6	9.0
M06-L	3.3	6.0	PW86reLYP	4.1	9.6
TPSSh	−2.3	6.2	C09SOGGA11	−6.4	9.9
TPSS	−0.6	6.2	GVWN3	1.8	10.0
MOHLYP	4.1	6.2	M05-2X	8.1	10.3
O3LYP	2.8	6.4	B88	−9.4	10.6
TPSS1KCIS	−2.0	6.4	M05	10.3	11.4
B3PW91	−3.9	6.4	N12-SX	9.9	11.6
PBE0	−5.1	6.5	M06-2X	8.9	12.2
PW91	0.0	6.8	HCTH	11.9	12.6
PBE	−0.6	6.8	MN12-L	11.6	12.9
BP86	0.9	6.8	M11-L	5.4	13.7
BMK	−1.2	6.9	LC-MPWLYP	12.6	14.7
C09reLYP	1.8	6.9	HFPW91	−12.7	15.1
ωB97X	6.9	7.0	M11	7.6	15.9
M06	5.4	7.1	HFLYP	−6.4	18.6
B97-2	6.0	7.2	πHCTH	18.9	19.3
C09LYP	0.5	7.2	HF	−20.4	23.3
BPW91	−1.6	7.3	N12	13.2	24.0
MPWLYP1M	3.6	7.4	MN12-SX	25.5	26.1
BLYP	3.7	7.5	M06-HF	15.9	27.0

Table 11. MSE(10) and MUE(10) for the Ionization Potentials (kcal/mol) for the Variational Method

functional	MSE	MUE	functional	MSE	MUE
B97-3	1.8	2.0	C09reLYP	4.2	6.3
B97-1	1.6	2.3	TPSSh	−1.9	6.3
B98	1.8	2.6	N12-SX	−4.3	6.3
ωB97X-D	−0.5	2.7	revTPSS	0.6	6.4
PW6B95	0.9	2.9	M06-HF	0.2	6.4
ωB97X	0.5	3.0	MN12-L	−3.7	6.4
B1LYP	1.6	3.4	TPSS	0.4	6.6
M08-SO	1.2	3.6	M11-L	−3.3	6.7
MPW1B95	−2.0	3.6	SOGGA11	3.0	6.8
B97-2	−1.7	3.6	SOGGA11-X	6.8	6.8
CAM-B3LYP	2.5	3.9	RPBE	2.9	6.9
B3V5LYP	3.0	4.3	M06	5.1	7.1
BHandHLYP	−0.6	4.3	MPWLYP1M	6.1	7.2
MPWB1K	−3.7	4.3	SOGGA	1.6	7.3
OreLYP	0.9	4.4	OPBE	−4.9	7.5
M08-HX	−3.5	4.5	LC-ωPBE	−7.0	7.7
τ-HCTHhyb	4.0	4.6	BLYP	6.0	7.8
LC-MPWLYP	−2.0	4.7	C09PBE	−2.1	7.9
O3LYP	−2.4	4.9	PW86SOGGA11	−3.6	8.0
MOHLYP	−1.3	5.0	HCTH	8.0	8.1
PBE0	−1.5	5.1	PBE	4.9	8.2
MPWKCIS1K	−4.6	5.1	mPWLYP	7.3	8.3
MPW3LYP	4.8	5.1	BPW91	3.9	8.5
BHandH	−3.1	5.3	N12	−5.7	8.5
B3LYP	4.9	5.4	PW91	6.2	8.9
τ-HCTH	3.9	5.5	M05-2X	7.1	9.1
BMK	4.5	5.5	HFLYP	−6.5	9.1
OLYP	−2.4	5.5	BP86	8.5	9.8
HSE	−0.8	5.6	PW86PBE	8.3	10.0
VS98	1.1	5.7	MN12-SX	−0.6	10.0
MPW1K	−3.9	5.7	PW86LYP	12.0	12.0
C09LYP	0.6	5.8	B88	−8.1	12.3
M06-L	1.0	5.8	HFPW91	−12.0	13.2
B3PW91	−0.1	5.9	C09SOGGA11	−13.6	14.9
M05	−0.5	5.9	M11	−16.3	16.3
M06-2X	5.2	5.9	PW86reLYP	16.4	16.4
TPSS1KCIS	−1.7	6.0	GVWN3	20.6	20.6
B3LYP*	5.5	6.2	HF	−25.7	25.7

energy. This produces excitation energies with errors like 50 or 100 kcal/mol. This problem is observed most often for M06-HF and MN12-L, for three or four cases each. Other functionals do not lead to this problem in such a serious way; nevertheless we recommend basing final conclusions in Table 15 (which excludes these two cases as discussed at the end of Section 4.2) rather than Table 14 to exclude the inappropriate cases for the RBS method.

As discussed at the end of Section 3, the present study also features tests of the performance of eight new GGAs formed from the PW86 and C09 exchange functionals. By combining them with PBE, LYP, reLYP, and SOGGA11, we create eight new GGAs for testing. Table 15 shows the disappointing performance of the resulting functionals, with the smallest error coming from C09reLYP, at 6.6 kcal/mol. By comparing results from C09LYP, C09reLYP, and C09PBE with OLYP, OreLYP, and OPBE, we conclude that C09 has comparable performance to OptX for 3d transition metals. For PW86, one also finds PW86PBE to be very similar errors to to OPBE, but the best performance for PW86 comes from combining it with the SOGGA11 correlation functional.

The seven highest-ranking functionals in Table 15, which in some sense is the culmination of the present study of the 3d-series of transition metals, are ωB97X-D, B97-3, M08-SO, MPW1B95, and B98, followed closely by PW6B95, CAM-B3LYP, MPWB1K, SOGGA11-X, and B97-1. These higher-performing functionals include four global-hybrid GGAs, four global-hybrid meta-GGAs, one long-range-corrected GGA, one long-range-corrected GGA plus molecular mechanics, and no local functionals of any kind (the highest local functional in Table 15 is M06-L). In the next section we examine these functionals plus the eight new functionals from a broader perspective.

5.3. Broader Comparisons. To achieve a broader conclusion about the overall performance of various functionals, in Table 16 we compare the results in this study of the 3d-series with the results for five previously considered databases. The functionals listed in Table 16 are limited to those in the top 15 for either the 3d- or the 4d-series database

dx.doi.org/10.1021/ct400712k | J. Chem. Theory Comput. XXXX, XXX, XXX−XXX

Table 12. MSE(10) and MUE(10) for the Ionization Potentials (kcal/mol) for the WABS Method

functional	MSE	MUE	functional	MSE	MUE
B97-3	1.8	2.1	TPSSh	−1.7	6.2
B97-1	1.7	2.3	B3LYP*	5.6	6.2
B98	1.8	2.6	C09reLYP	4.2	6.2
ωB97X-D	−0.5	2.7	MN12-L	−3.8	6.2
PW6B95	0.9	2.9	N12-SX	−4.3	6.3
ωB97X	0.5	3.1	TPSS	0.5	6.4
B1LYP	1.7	3.4	RPBE	3.1	6.6
M08-SO	1.2	3.6	SOGGA11	3.2	6.7
MPW1B95	−2.0	3.6	SOGGA11-X	6.8	6.8
B97-2	−1.7	3.6	M06	5.2	7.0
CAM-B3LYP	2.5	3.9	M11-L	−2.8	7.1
OreLYP	1.1	4.2	MPWLYP1M	6.2	7.1
B3V5LYP	3.1	4.3	SOGGA	1.8	7.2
BHandHLYP	−0.5	4.3	OPBE	−4.6	7.3
MPWB1K	−3.7	4.3	BLYP	6.1	7.6
M08-HX	−3.5	4.5	LC-ωPBE	−6.9	7.7
LC-MPWLYP	−2.0	4.7	C09PBE	−2.0	7.8
τ-HCTHhyb	4.1	4.7	PW86SOGGA11	−3.5	8.0
O3LYP	−2.2	4.7	PBE	5.0	8.0
MOHLYP	−1.1	4.7	mPWLYP	7.4	8.2
PBE0	−1.4	5.0	M06-HF	−1.3	8.2
MPWKCIS1K	−4.6	5.1	BPW91	4.0	8.3
MPW3LYP	4.8	5.1	HCTH	8.5	8.5
M06-L	1.5	5.2	N12	−5.7	8.6
OLYP	−2.1	5.3	PW91	6.3	8.7
BHandH	−3.1	5.3	M05-2X	7.1	8.9
B3LYP	4.9	5.4	HFLYP	−6.5	9.1
BMK	4.5	5.5	BP86	8.6	9.7
HSE	−0.8	5.5	MN12-SX	−0.4	9.8
VS98	1.1	5.6	PW86PBE	8.4	9.9
C09LYP	0.7	5.6	B88	−8.1	12.1
MPW1K	−3.9	5.7	PW86LYP	12.1	12.1
M06-2X	5.1	5.8	HFPW91	−12.0	13.2
τ-HCTH	4.7	5.8	C09SOGGA11	−13.5	14.8
B3PW91	0.0	5.8	M11	−16.3	16.3
M05	−0.5	5.8	PW86reLYP	16.4	16.4
TPSS1KCIS	−1.6	5.9	GVWN3	20.6	20.6
revTPSS	0.7	6.1	HF	−25.6	25.6

Table 13. MSE(10) and MUE(10) for the Ionization Potentials (kcal/mol) for the RBS Method

functional	MSE	MUE	functional	MSE	MUE
B97-3	1.8	2.1	MN12-L	−3.7	6.2
B97-1	1.7	2.3	B3LYP*	5.6	6.2
B98	1.9	2.5	C09reLYP	4.2	6.2
ωB97X-D	−0.5	2.7	M06-2X	5.3	6.4
ωB97X	0.5	3.1	N12-SX	−4.3	6.4
B97-2	−1.5	3.5	SOGGA11-X	6.7	6.7
MPW1B95	−2.0	3.6	M06	5.4	6.8
OreLYP	2.2	3.7	OPBE	−4.2	6.8
CAM-B3LYP	2.6	3.9	SOGGA	2.1	6.9
MOHLYP	−0.6	4.0	MPWLYP1M	6.3	6.9
M08-SO	2.5	4.1	BLYP	6.2	6.9
B3V5LYP	3.1	4.3	SOGGA11	3.6	7.1
MPWB1K	−3.6	4.3	M11-L	−2.2	7.2
O3LYP	−1.9	4.4	τ-HCTH	6.4	7.4
M06-L	1.8	4.4	PBE	5.4	7.4
OLYP	−1.3	4.6	BPW91	4.2	7.7
PW6B95	2.7	4.6	C09PBE	−2.0	7.8
B1LYP	3.1	4.8	mPWLYP	7.5	7.9
τ-HCTHhyb	4.2	4.8	PW86SOGGA11	−3.5	8.0
PBE0	−1.4	5.0	LC-ωPBE	−6.6	8.2
MPWKCIS1K	−4.6	5.1	PW91	6.7	8.3
MPW3LYP	4.8	5.2	M05-2X	6.8	8.4
BHandH	−3.1	5.3	HCTH	9.1	9.1
VS98	1.0	5.3	MN12-SX	2.2	9.3
BHandHLYP	−1.6	5.4	BP86	9.1	9.3
B3LYP	5.0	5.4	HFLYP	−6.8	9.3
HSE	−0.7	5.5	PW86PBE	8.4	9.9
BMK	4.5	5.5	B88	−8.4	11.1
M05	−0.6	5.5	PW86LYP	12.1	12.1
revTPSS	0.8	5.6	HFPW91	−12.0	13.2
C09LYP	0.7	5.6	C09SOGGA11	−13.5	14.8
MPW1K	−3.9	5.6	PW86reLYP	16.4	16.4
RPBE	3.6	5.6	LC-MPWLYP	11.9	18.6
TPSS1KCIS	−1.3	5.6	M11	−12.7	19.8
M08-HX	−3.3	5.7	GVWN3	20.6	20.6
TPSS	0.9	5.7	N12	4.1	22.2
B3PW91	0.1	5.7	HF	−25.5	25.5
TPSSh	−1.4	5.9	M06-HF	−6.8	31.1

plus the eight new functionals, plus SOGGA11 because it is of special interest to compare it to the eight new functionals and M06 because of its generally good performance across a broad spectrum of problems. The first six numerical columns give the MUE for each of the six considered databases, namely, in order, the MUE(28) of the RBS column of Table 15, the MUE(22) for spin-state excitation energies and ionization potentials of 4d-series atoms and monatomic cations from ref 6, MUE(VR17) for p-block spin-state excitation energies from Table 7 of ref 5, and AE6/11, PPS5/05, and ABDE12 from a recent review[96] of respectively main-group atomization energies, alkyl bond dissociation energies, and noncovalent $\pi-\pi$ interaction energies. In some cases those earlier compilations did not include all the functionals in Table 16, and so the missing results were calculated as part of the present work, specifically for this comparison.

The next four columns of Table 16 show the average MUE of the first two, three, four, or five databases in Table 16, and the final column shows the average over all six. These results are labeled AMUE$x(y)$, where x is the number of MUEs averaged, and y is the total number of data in the x databases. Note that these are averages over MUEs, not averages over the collected data; averages over MUEs have the effect of weighting the six databases more evenly than would be the case if we averaged over data because the various databases have greatly different numbers of data. The functionals in Table 16 are listed in order of increasing values in this last column. Of course a complete assessment would require that even more databases be considered,[4,6,96−99] but that is the job for a review article. Here we simply consider six databases to show which of the functionals that do well in Table 15 or in the closely related study of the 4d-series also do well across a broader spectrum of data and to provide a comparison of the new functionals to other functionals across a broader spectrum than just the 3d transition series atoms.

Consider first AMUE2(39), which merges the assessments for the 3d-series with those for the 4d-series. This provides the most comprehensive available assessment of spin excitation energies and ionization potentials for d-block atoms and cations. We find that SOGGA11-X, a functional with the same

dx.doi.org/10.1021/ct400712k | J. Chem. Theory Comput. XXXX, XXX, XXX−XXX

Table 14. MUE(30)[a]

functional	var (kcal/mol)	WABS (kcal/mol)	RBS (kcal/mol)	functional	var (kcal/mol)	WABS (kcal/mol)	RBS (kcal/mol)
SOGGA11-X	6.2	4.8	3.6	ωB97X	5.0	6.0	7.1
ωB97X-D	3.7	4.4	4.3	B97-2	5.9	6.6	7.2
MPW1B95	4.1	4.3	4.5	M06	7.8	7.5	7.2
MPWB1K	5.3	4.8	4.6	M08-HX	4.6	4.9	7.4
C09reLYP	6.7	7.4	4.6	BPW91	8.4	8.2	7.4
C09LYP	6.7	7.1	4.8	MPWLYP1M	7.1	8.1	7.5
B97-3	3.3	4.5	4.9	BLYP	7.6	8.5	7.7
CAM-B3LYP	4.2	5.2	5.1	HSE	6.8	6.7	7.8
M08-SO	4.4	4.1	5.2	OLYP	7.3	7.9	8.0
PW86PBE	8.5	8.5	5.2	SOGGA	8.2	7.9	8.1
PW6B95	3.8	4.4	5.2	VS98	7.8	7.3	8.2
B3V5LYP	4.7	5.8	5.3	mPWLYP	7.9	8.8	8.2
B3LYP	5.1	6.2	5.4	MPWKCIS1K	6.3	6.1	8.4
PW86SOGGA11	8.1	8.7	5.5	τ-HCTHhyb	7.0	7.7	8.5
B98	4.2	5.2	5.5	BHandHLYP	7.5	7.1	8.6
B1LYP	4.1	5.2	5.6	MPW1K	8.6	7.3	8.7
MPW3LYP	4.8	6.1	5.7	LC-ωPBE	7.7	7.6	8.7
PW86LYP	9.7	10.1	5.7	SOGGA11	8.1	7.9	8.7
B97-1	4.2	5.3	5.8	OreLYP	7.0	7.6	8.8
BHandH	6.6	6.3	5.8	OPBE	9.3	9.2	8.9
B3LYP*	5.8	6.8	5.9	GVWN3	13.9	13.9	10.2
C09PBE	8.6	8.4	6.0	M05-2X	10.9	9.9	10.5
RPBE	6.8	7.1	6.1	B88	12.8	11.8	11.0
revTPSS	6.7	6.8	6.1	M05	9.6	9.5	11.4
M06-L	6.8	6.3	6.1	N12-SX	9.4	9.9	11.7
TPSSh	6.7	6.7	6.3	LC-MPWLYP	5.5	6.3	12.2
TPSS	6.9	7.1	6.3	M06-2X	9.3	8.7	12.2
MOHLYP	6.0	6.8	6.4	HCTH	10.1	10.7	12.6
O3LYP	5.7	6.5	6.4	MN12-L	10.0	10.1	13.1
PW86reLYP	11.9	12.1	6.4	M11-L	11.7	11.8	13.9
TPSS1KCIS	6.6	6.7	6.5	M11	10.6	11.3	14.8
B3PW91	6.7	6.5	6.5	HFPW91	17.0	15.4	15.2
C09SOGGA11	11.6	10.9	6.6	HFLYP	17.9	15.9	18.6
PBE0	6.2	6.2	6.7	τ-HCTH	12.8	13.2	19.4
BMK	7.3	6.9	6.9	N12	13.6	13.4	22.1
PW91	8.2	8.2	6.9	HF	26.8	24.5	23.3
PBE	7.9	7.8	6.9	M06-HF	17.7	17.0	25.7
BP86	8.1	8.5	6.9	MN12-SX	15.8	15.7	25.8

[a]MUE(30) is in kcal/mol. The functionals are arranged in order of increasing MUE for the RBS method. When the MUE for RBS is the same (rounded to the nearest tenth of a kcal/mol), the order is the sum of the MUs for the variational, WABS, and RBS methods.

ingredients as the popular and historically important B3LYP functional, does the best. This is a fairly recent functional, and it is encouraging that a recently parametrized functional does so well. This is even more encouraging when we note that the data in the 3d- and 4d-series and p-block databases are quite different than the data used for parametrization in any of the parametrized functionals. The second- and third-best functionals for the AMUE2(39) figure of merit are CAM-B3LYP and B1LYP, followed closely by PW6B95 and B3V5LYP.

Next consider AMUE3(67), which adds in the p-block results for spin-state excitation energies. The p-block database includes both valence and Rydberg excitations of atoms in the 2p, 3p, and 4p blocks. Over this broader database, which now includes a wide expanse of the periodic table, the best performing functional becomes PW6B95 (whose design involved the optimization of only six parameters), followed by MPW1B95 (which was created by optimizing only one parameter) and CAM-B3LYP.

PW6B95 remains the best functional for AMUE4(73) and AMUE5(85). The good performance of PW6B95 when averaged over the three, four, or five databases culminating in AMUE5(85) is very interesting because Grimme, in several studies, has noted the especially good performance of this functional (sometimes augmented by molecular mechanics terms) on broad data sets of thermochemical data,[98−102] which although broad and diverse are quite different from the p-block and d-block atomic data considered here.

The last column of Table 16 provides the broadest assessment considered in the present paper. Although one might have recommended functionals such as B3V5LYP, B1LYP, and B97-1 due to their good performances in spin state and ionization potential tests, we find they fail to deliver consistently best accuracy when broader data are considered. M08-SO and PW6B95 do best, followed closely by MPW1B95, MPWB1K, SOGGA11-X, and CAM-B3LYP, but a key point is that 11 of the functionals that made their way into Table 16 by good performance on the 3d- or 4d-series databases of atomic

dx.doi.org/10.1021/ct400712k | J. Chem. Theory Comput. XXXX, XXX, XXX−XXX

Table 15. MUE(28)[a]

functional	var (kcal/mol)	WABS (kcal/mol)	RBS (kcal/mol)	functional	var (kcal/mol)	WABS (kcal/mol)	RBS (kcal/mol)
ωB97X-D	4.4	3.9	3.8	τ-HCTHhyb	7.7	7.3	7.3
B97-3	4.6	3.4	3.9	VS98	7.5	8.0	7.3
M08-SO	4.2	4.4	4.2	MPWLYP1M	8.2	7.2	7.4
MPW1B95	4.2	4.3	4.3	BHandHLYP	7.1	6.5	7.5
B98	5.2	4.4	4.5	PW91	8.5	8.5	7.6
PW6B95	4.3	4.0	4.6	BLYP	8.7	7.7	7.6
CAM-B3LYP	5.2	4.4	4.6	BPW91	8.5	8.7	7.7
B97-1	5.3	4.5	4.7	MPW1K	7.7	8.5	7.9
MPWB1K	5.1	5.0	4.7	SOGGA	8.1	8.5	7.9
SOGGA11X	4.8	5.4	4.7	BP86	8.8	8.4	8.0
B1LYP	5.3	4.1	5.0	SOGGA11	8.2	8.2	8.0
B3V5LYP	5.8	4.9	5.0	PW86SOGGA11	8.6	7.9	8.1
B3LYP	6.3	5.3	5.5	mPWLYP	9.1	8.0	8.3
MPW3LYP	6.1	5.1	5.6	LC-ωPBE	7.7	8.0	8.4
M06-L	6.6	6.2	5.6	OPBE	9.5	9.7	8.4
MOHLYP	7.0	6.1	5.6	PW86PBE	8.8	8.8	8.5
ωB97X	6.1	5.3	5.7	C09PBE	8.7	9.0	8.6
O3LYP	6.5	5.8	5.7	M05	9.5	9.8	9.4
BHandH	6.4	5.8	5.7	PW86LYP	10.7	9.8	9.8
B97-2	6.6	6.2	5.9	N12-SX	9.9	9.6	9.9
B3LYP*	6.8	5.9	6.0	M05-2X	10.1	9.9	10.0
RPBE	7.3	7.0	6.1	M06-2X	9.3	9.3	10.3
revTPSS	7.1	6.8	6.1	MN12-L	10.7	10.0	10.8
TPSS	7.4	7.0	6.2	LC-MPWLYP	6.1	5.4	11.3
PBE0	6.3	6.6	6.3	HCTH	11.0	10.8	11.3
BMK	6.9	6.3	6.3	B88	12.5	13.2	11.5
TPSSh	6.9	6.8	6.3	C09SOGGA11	11.5	11.7	11.7
TPSS1KCIS	6.8	6.7	6.3	M11-L	11.7	11.3	11.8
M08-HX	5.1	4.6	6.3	PW86reLYP	12.6	11.6	12.1
B3PW91	6.6	6.9	6.4	GVWN3	14.5	14.7	14.3
C09reLYP	7.3	6.9	6.6	HFPW91	14.9	14.7	14.5
C09LYP	7.6	6.9	6.7	M11	11.4	10.9	15.2
OLYP	8.2	7.5	6.8	τ-HCTH	13.4	13.4	15.2
OreLYP	7.9	7.1	7.1	HFLYP	15.1	15.1	15.3
MPWKCIS1K	6.0	6.4	7.1	MN12-SX	16.7	16.3	19.5
HSE	6.7	7.0	7.1	N12	13.7	14.2	19.8
M06	7.6	8.2	7.2	HF	24.4	24.8	24.0
PBE	8.0	8.2	7.3	M06-HF	17.1	18.8	25.9

[a]MUE(28) is in kcal/mol. The functionals are arranged in order of increasing MUE for the RBS method. When the MUE for RBS is the same (rounded to the nearest tenth of a kcal/mol), the order is the sum of the MUs for the variational, WABS, and RBS methods.

spin-state excitation energies and ionization potentials have average MUEs larger than those of the best functionals in Table 16 by a factor of 1.5 or more when assessed broadly. So a prospective user of these functionals should consider more than one kind of database when choosing a functional for a series of applications.

Table 16 also clearly shows the disappointing performance of the PW86 and C09 exchange functionals in treating the wider range of systems in that the eight new functionals occupy the eight lowest positions in the table. A somewhat surprising observation is their poor performance on PPS/5 since they are meant to be more accurate for weak interactions. Overall one finds the error of even the best of the four, namely, PW86PBE, to be 7.0 kcal/mol, more than twice as large as the errors of the top 5 functionals in the table. It is also interesting to note that none of these functionals does as well as SOGGA11, whose exchange functional shares the major characteristic of the PW86 and C09 exchange functionals, i.e., good agreement with the exact gradient expansion at small values of the reduced gradient. To the knowledge of the authors, the present study is the broadest available test of the PW86 and C09 functionals, and it seems safe to exclude both from the list of exchange functionals recommended for use in GGAs for general applications in chemistry.

Note that, excluding the eight new functionals, only three local functionals are included in Table 16, namely, revTPSS and M06-L, which are both meta-GGA functionals, and SOGGA11, which is a GGA. Among these, revTPSS has the best overall accuracy (4.4 kcal/mol). The older M06-L functional does better than revTPSS on four of the six databases but is ranked lower in Table 16 primarily because of poor performance for open-shell p-block states, in particular for the Rydberg state component of that database. SOGGA11, with one less ingredient than M06-L or revTPSS, does better than former on two of the six databases and does better than the latter on two of the six databases (not the same two).

Table 16. Summary of Overall MUE (kcal/mol) of 19 Functionals for 6 Databases[a]

	3d	4d	p	AE6/11	ABDE12	PPS5/05	AMUE2(39)[b]	AMUE3(67)[c]	AMUE4(73)[d]	AMUE5(85)[e]	AMUE6(90)[f]
M08-SO	4.2	5.4	4.2	0.4	3.4	0.3	4.8	4.6	3.5	3.5	3.0
PW6B95	4.6	3.7	3.2	0.4	5.4	0.8	4.2	3.8	3.0	3.5	3.0
MPW1B95	4.3	4.3	3.4	0.8	4.6	1.1	4.3	4.0	3.2	3.5	3.1
MPWB1K	4.7	5.2	3.5	1.1	4.8	0.7	5.0	4.5	3.6	3.8	3.3
SOGGA11-X	4.7	3.1	5.5	0.7	5.0	2.1	3.9	4.4	3.5	3.8	3.5
CAM-B3LYP	4.6	3.6	3.9	0.4	7.4	1.9	4.1	4.0	3.1	4.0	3.6
BMK	6.3	3.7	6.5	0.5	3.8	2.4	5.0	5.5	4.2	4.1	3.9
ωB97X-D	3.8	5.9	8.1	0.4	4.5	0.7	4.9	5.9	4.5	4.5	3.9
B97-3	3.9	5.2	4.9	0.6	6.7	2.3	4.6	4.7	3.7	4.3	3.9
B98	4.5	5.1	4.6	0.7	6.8	2.0	4.8	4.7	3.7	4.3	3.9
MPW3LYP	5.6	3.5	4.7	0.3	8.5	2.0	4.6	4.6	3.5	4.5	4.1
revTPSS	6.1	4.5	3.5	1.2	8.6	2.5	5.3	4.7	3.8	4.8	4.4
B3LYP	5.5	3.6	4.1	0.8	9.8	2.9	4.6	4.4	3.5	4.8	4.4
B3LYP*	5.5	3.6	3.4	3.1	8.3	2.8	4.6	4.2	3.9	4.8	4.5
TPSS1KCIS	6.3	4.1	3.8	0.6	9.7	2.3	5.2	4.7	3.7	4.9	4.5
MPWKCIS1K	7.1	4.3	4.0	1.6	8.0	1.8	5.7	5.1	4.3	5.0	4.5
B97-1	4.7	5.9	5.0	4.6	5.8	1.7	5.3	5.2	5.0	5.2	4.6
TPSSh	6.3	4.2	3.2	1.2	10.5	2.5	5.3	4.6	3.7	5.1	4.6
SOGGA11	8.0	6.8	4.8	1.8	6.9	0.4	7.4	6.5	5.3	5.7	4.8
M06	7.2	8.8	8.4	0.5	4.1	0.2	8.0	8.1	6.2	5.8	4.9
M06-L	5.6	6.3	9.3	0.6	7.8	0.2	6.0	7.1	5.5	5.9	5.0
B1LYP	5.0	3.1	4.6	2.7	11.6	2.9	4.1	4.2	3.8	5.4	5.0
B3V5LYP	5.0	3.3	4.2	4.9	10.2	2.9	4.2	4.2	4.4	5.5	5.1
MOHLYP	5.6	4.0	5.0	2.3	14.9	6.1	4.8	4.9	4.2	6.4	6.3
BHandH	5.7	3.9	3.7	21.9	5.0	1.0	4.8	4.4	8.8	8.0	6.9
PW86PBE	8.5	6.2	6.9	7.6	10.2	2.5	7.4	7.2	7.3	7.9	7.0
C09LYP	6.7	4.9	5.1	22.7	3.9	3.2	5.8	5.5	9.8	8.6	7.7
PW86LYP	9.8	6.1	11.4	6.7	12.0	2.3	8.0	9.1	8.5	9.2	8.1
C09reLYP	6.6	4.3	6.1	26.5	3.9	3.6	5.5	5.7	10.9	9.5	8.5
PW86reLYP	12.1	7.6	12.8	5.5	11.8	2.7	9.8	10.8	9.5	9.9	8.7
C09PBE	8.6	7.3	6.1	29.4	3.9	3.5	7.9	7.3	12.8	11.1	9.8
C09SOGGA11	11.7	11.0	4.2	30.1	22.6	9.3	11.4	9.0	14.2	15.9	14.8
PW86SOGGA11	8.1	8.1	5.6	56.8	32.4	8.6	8.1	7.3	19.6	22.2	19.9

[a]MUE is in kcal/mol. [b]Averaged over columns 3d and 4d. [c]Averaged over column 3d, 4d, and p. [d]Averaged over column 3d, 4d, p, and AE6/11. [e]Averaged over column 3d, 4d, p, AE6/11, and ABDE12. [f]Averaged over columns 3d, 4d, p, AE6/11, ABDE12, and PPS5/05.

6. SUMMARY AND CONCLUSIONS

The present article tests 75 density functionals for excitation energies and ionization potentials of all 3d transition-metal atoms and their monocations. The results for 33 of the xc functionals are systematically compared to results obtained for five other databases of accurate comparison data, including excitation energies and ionization potentials for the 4d transition-metal atoms and cations, for which we find different performances, illustrating the difficulty of obtaining a universally accurate functional and the need for broad-based testing. The databases chosen for the tests have been very carefully vetted and include only highly reliable data.

The xc functionals in this paper are drawn from six classes of local functionals, in particular, LSDA, GGA, NGA, meta-GGA, range-separated meta-GGA, and meta-NGA, and from eight classes of hybrid functionals, in particular, global-hybrid GGA, global-hybrid meta-GGA, long-range-corrected GGA, long-range-corrected meta-GGA, screened exchange GGA, screened exchange NGA, screened exchange meta-NGA, and long-range-corrected GGA. No single available software package has all the functionals studied in this paper. The present paper includes not only tests for 3d transition metals of the most popular, most accurate, and most fundamentally interesting functionals from previous work but also eight new functionals containing the recently popular PW96 exchange functional and the recently proposed C09 exchange functional, and these are tested not only against the data for 3d transion metals but also against the five other databases spanning a broad range of chemistry.

In addition to the tests of functionals against databases, the article includes a fundamental analysis of the broken-symmetry problem that arises in many applications of DFT to open-shell systems. As a result of that analysis, we present a more justifiable method (called the reinterpreted broken-symmetry method) for handing open-shall systems and test it.

Several interesting observations can be made about the excitation energies and ionization potentials of the 3d-series transition-metal atoms and their monatomic cations: In contrast to a common belief that local functionals perform better than hybrid functionals for multireference systems, such as transition-metal atoms, this work found that an appropriate percentage of Hartree−Fock exchange is necessary for a balanced description of s and d orbitals, as needed for high accuracy of calculations of excitation energies and ionization potentials.

We have tested the new way, called RBS, to treat broken-symmetry systems, and its performance is generally on par with the popular WABS method, although one can argue that RBS is

more physically justified. This method opens a new approach to resolve the broken-symmetry problem, and its usefulness still requires further testing in applications. Generally, we find that RBS and WABS provide improved performance for most broken-symmetry problems, and thus they should be applied in preference to the straight variational method whenever appropriate.

The B97-x series of xc functionals, which are specifically parametrized for transition-metal systems, showed very good performance in our tests. The ωB97X-D functional is the only functional that does better than B97-3 for the spin-state excitation energies and ionization potentials in the 3d-series (Table 15). When we average over the 3d- and 4d-series (with results summarized by the AMUE2(39) column of Table 16), six functionals do better than B97-3, namely SOGGA11-X, CAM-B3LYP, B1LYP, PW6B95, B3V5LYP, and MPW1B95; and B3LYP*, B3LYP, and MPW3LYP do as well as B97-3.

Although the top 16 functionals in the first summary table (Table 14) and the top14 functionals in the second summary table (Table 15) have nonzero Hartree−Fock exchange, in both cases the next functional is the local M06-L; thus for larger systems where a local functional is computationally advantageous, M06-L, as verified by many previous studies,[69,70,103,104] is our best candidate for treatment of 3d transition metals. Four other local functionals do almost as well though for the 3d-series transition metals and monatomic cations, namely MOHLYP, revTPSS, RPBE, and TPSS, which can also be recommended for this kind of application.

The comparisons on the broader test sets including only xc functionals ranked near the top for the 3d-series atoms and monatomic ions or the 4d-series atoms and monatomic ions (or both) plus the eight totally new functionals and two functionals of special interest. By comparing the AMUE of 23 top performers, we find PW6B95, MPW1B95, CAM-B3LYP, B3V5LYP, and B1LYP to be most accurate for calculations of spin states and ionization potentials of p-block and 3d- and 4d-series elements.

Broadening the examination of these functionals even further to include three other databases, in particular main-group atomization energies, alkyl bond dissociation energies, and noncovalent $\pi-\pi$ interaction energies, we found that PW6B95, MPW1B95, M08-SO, MPWB1K, and SOGGA11-X are the best five functionals for a more balanced treatment of spin states, thermodynamic energies, and noncovalent interactions. Because of the importance of accuracy across a broad range of properties in transition-metal studies, we highly recommend these five xc functionals for a variety of applications

As a final comment we return to a point made at the end of the introduction, as stated from another point of view by Harvey,[105] namely that an "objection to the use of atoms as reference systems is that their electronic structure is often not typical of that of the metallic complexes for which prediction of spin states is desirable [for applications]." This "objection" also applies to small molecules with highly unsaturated valences; in fact, problems such as considered in this article and some of our previous work are more challenging than the usual test cases, and some xc functionals may do better for closed-shell or nearly closed-shell compounds than for atoms. For that reason, though, one could argue that tests on atoms are particularly important test cases at the very boundary of where KS DFT with presently available functionals may be applied; and tests on atoms eliminate some sources of cancellation of errors, such as a tendency to produced too delocalized or too ionic bonds. Furthermore, if one is interested in bonding and bond energies, it is reasonable to ask that the theory be equally applicable to the atomic bonding partners as to the resultant bonded molecule. Our attitude is that examining the performance of DFT on all kinds of systems is essential if one is to pursue the goal of achieving a more universally valid xc functional, and we assembled the present set of test calculations as part of the background information needed for designing improved functionals as well as for guiding and validating applications based on currently available functionals.

AUTHOR INFORMATION

Corresponding Author

*E-mail: truhlar@umn.edu.

Present Address

[†]Boris Averkiev, Institute for Shock Physics, Washington State University, Pullman, WA 99164−2816

Notes

The authors declare no competing financial interest.

ACKNOWLEDGMENTS

The authors are grateful to Yan Zhao for contributions to this project. This work was supported in part by the Air Force Office of Scientific Research under grant no. FA9550-11-1-0078.

REFERENCES

(1) Kohn, W.; Sham, L. J. *Phys. Rev.* **1965**, *140*, A1133.
(2) Reiher, M. *Faraday Discuss.* **2007**, *135*, 97.
(3) Jacob, C. R.; Reiher, M. *Int. J. Quantum Chem.* **2012**, *112*, 3661.
(4) Cramer, C. J.; Truhlar, D. G. *Phys. Chem. Chem. Phys.* **2009**, *11*, 10757.
(5) Yang, K.; Peverati, R.; Truhlar, D. G.; Valero, R. *J. Chem. Phys.* **2011**, *135*, 044118.
(6) Luo, S.; Truhlar, D. G. *J. Chem. Theory Comput.* **2012**, *8*, 4112.
(7) Frisch, M. J.; Trucks, G. W.; Schlegel, H. B. Scuseria, G. E.; Robb, M. A.; Cheeseman, J. R.; Scalmani, G.; Barone, V.; Mennucci, B.; Petersson, G. A.; Nakatsuji, H.; Caricato, M.; Li, X.; Hratchian, H. P.; Izmaylov, A. F.; Bloino, J.; Zheng, G.; Sonnenberg, J. L.; Hada, M.; Ehara, M.; Toyota, K.; Fukuda, R.; Hasegawa, J.; Ishida, M.; Nakajima, T.; Honda, Y.; Kitao, O.; Nakai, H.; Vreven, T.; Montgomery, J. A., Jr.; Peralta, J. E.; Ogliaro, F.; Bearpark, M.; Heyd, J. J.; Brothers, E.; Kudin, K. N.; Staroverov, V. N.; Kobayashi, R.; Normand, J.; Raghavachari, K.; Rendell, A.; Burant, J. C.; Iyengar, S. S.; Tomasi, J.; Cossi, M.; Rega, N.; Millam, J. M.; Klene, M.; Knox, J. E.; Cross, J. B.; Bakken, V.; Adamo, C.; Jaramillo, J.; Gomperts, R.; Stratmann, R. E.; Yazyev, O.; Austin, A. J.; Cammi, R.; Pomelli, C.; Ochterski, J. W.; Martin, R. L.; Morokuma, K.; Zakrzewski, V. G.; Voth, G. A.; Salvador, P.; Dannenberg, J. J.; Dapprich, S.; Daniels, A. D.; Farkas, Ö.; Foresman, J. B.; Ortiz, J. V.; Cioslowski, J.; Fox, D. J. *Gaussian 09*, revision C.1; Gaussian, Inc.: Wallingford, CT, 2009.
(8) Balabanov, N. B.; Peterson, K. A. *J. Chem. Phys.* **2005**, *123*, 064107.
(9) Douglas, M.; Kroll, N. M. *Ann. Phys.* **1974**, *82*, 89.
(10) Hess, B. A. *Phys. Rev. A* **1986**, *33*, 3742.
(11) Jansen, G.; Hess, B. A. *Phys. Rev. A* **1989**, *39*, 6016.
(12) Foster, J. P.; Weinhold, F. *J. Am. Chem. Soc.* **1980**, *102*, 7211.
(13) Reed, A. E.; Weinhold, F. *J. Chem. Phys.* **1983**, *78*, 4066.
(14) Reed, A. E.; Weinstock, R. B.; Weinhold, F. *J. Chem. Phys.* **1985**, *83*, 735.
(15) Reed, A. E.; Weinhold, F. *J. Chem. Phys.* **1985**, *83*, 1736.
(16) Carpenter, J. E. Ph. D. Thesis, University of Wisconsin, Madison, WI, 1987.
(17) Carpenter, J. E.; Weinhold, F. *J. Mol. Struct. (Theochem)* **1988**, *46*, 41.

(18) Reed, A. E.; Curtiss, L. A.; Weinhold, F. *Chem. Rev.* **1988**, *88*, 899.
(19) Weinhold, F.; Carpenter, J. E. In *The Structure of Small Molecules and Ions*; Naaman, R., Vager, Z., Eds.; Plenum: New York, 1988, pp 227−36.
(20) Moore, C. E. *Atomic Energy Levels*; National Bureau of Standards: Washington, DC, 1949−1958, Vols. *1*−*3*.
(21) Roothaan, C. C. J. *Rev. Mod. Phys.* **1951**, *23*, 69.
(22) Pople, J. A.; Nesbet, R. K. *J. Chem. Phys.* **1954**, *22*, 571.
(23) McWeeny, R.; Diercksen, G. *J. Chem. Phys.* **1968**, *49*, 4852.
(24) Becke, A. D. *J. Chem. Phys.* **1998**, *107*, 8554.
(25) Gáspár, R. *Acta Phys. Hung.* **1974**, *35*, 213.
(26) Vosko, S. H.; Wilk, L.; Nusair, M. *Can. J. Phys.* **1980**, *58*, 1200.
(27) Becke, A. D. *Phys. Rev. A* **1988**, *38*, 3098.
(28) Perdew, J. P. *Phys. Rev. B* **1986**, *33*, 8822.
(29) Lee, C.; Yang, W.; Parr, R. G. *Phys. Rev. B* **1988**, *37*, 785.
(30) Perdew, J. P. In *Electronic Structure of Solids '91*; Ziesche, P., Eschrig, H., Eds.; Akademie Verlag: Berlin, 1991, pp 11−20.
(31) Perdew, J. P.; Burke, K.; Ernzerhof, M. *Phys. Rev. Lett.* **1996**, *77*, 3865.
(32) Adamo, C.; Barone, V. *J. Chem. Phys.* **1998**, *108*, 664.
(33) Hamprecht, F. A.; Cohen, A.; Tozer, D. J.; Handy, N. C. *J. Chem. Phys.* **1998**, *109*, 6264.
(34) Boese, A. D.; Handy, N. C. *J. Chem. Phys.* **2001**, *114*, 5497.
(35) Hammer, B.; Hansen, L. B.; Norskov, J. K. *Phys. Rev. B* **1999**, *59*, 7413.
(36) Handy, N. C.; Cohen, A. J. *Mol. Phys.* **2001**, *99*, 403.
(37) Schultz, N. E.; Zhao, Y.; Truhlar, D. G. *J. Phys. Chem. A* **2005**, *109*, 11127.
(38) Thakkar, A. J.; McCarthy, S. P. *J. Chem. Phys.* **2009**, *131*, 134109.
(39) Peverati, R.; Truhlar, D. G. *J. Chem. Theory Comput.* **2012**, *8*, 2310.
(40) Van Voorhis, T.; Scuseria, G. E. *J. Chem. Phys.* **1998**, *109*, 400.
(41) Tao, J.; Perdew, J. P.; Staroverov, V. N.; Scuseria, G. E. *Phys. Rev. Lett.* **2003**, *91*, 146401.
(42) Zhao, Y.; Truhlar, D. G. *J. Chem. Phys.* **2006**, *125*, 194101.
(43) Zhao, Y.; Truhlar, D. G. *J. Chem. Phys.* **2008**, *128*, 184109.
(44) Perdew, J. P.; Ruzsinszky, A.; Csonka, G. I.; Constantin, L. A.; Sun, J. *Phys. Rev. Lett.* **2009**, *103*, 026403.
(45) Peverati, R.; Zhao, Y.; Truhlar, D. G. *J. Phys. Chem. Lett.* **2011**, *2*, 1911.
(46) Peverati, R.; Truhlar, D. G. *J. Phys. Chem. Lett.* **2011**, *2*, 2810.
(47) Peverati, R.; Truhlar, D. G. *Phys. Chem. Chem. Phys.* **2012**, *14*, 13171.
(48) Hoe, M. W.; Cohen, A. J.; Handy, N. C. *Chem. Phys. Lett.* **2001**, *341*, 319.
(49) Reiher, M.; Salomon, O.; Hess, B. A. *Theor. Chem. Acc.* **2001**, *107*, 48.
(50) Becke, A. D. *J. Chem. Phys.* **1993**, *98*, 1372.
(51) Stephens, P. J.; Devlin; Chabalowski, C. F.; Frisch, M. J. *J. Phys. Chem.* **1994**, *98*, 11623.
(52) Hartwig, R. H.; Koch, W. *Chem. Phys. Lett.* **1997**, *268*, 345.
(53) Zhao, Y.; Truhlar, D. G. *J. Phys. Chem. A* **2004**, *108*, 6908.
(54) Schmider, H. L.; Becke, A. D. *J. Chem. Phys.* **1998**, *108*, 9624.
(55) Adamo, C.; Barone, V. *J. Chem. Phys.* **1999**, *110*, 6158.
(56) Adamo, C.; Barone, V. *Chem. Phys. Lett.* **1997**, *274*, 242.
(57) Hamprecht, F. A.; Cohen, A.; Tozer, D. J.; Handy, N. C. *J. Chem. Phys.* **1998**, *109*, 6264.
(58) Wilson, P. J.; Bradley, T. J.; Tozer, D. J. *J. Chem. Phys.* **2001**, *115*, 9233.
(59) Keal, T. W.; Tozer, D. J. *J. Chem. Phys.* **2005**, *123*, 121103.
(60) Peverati, R.; Truhlar, D. G. *J. Chem. Phys.* **2011**, *135*, 191102.
(61) Lynch, B. J.; Fast, P. L.; Harris, M.; Truhlar, D. G. *J. Phys. Chem. A* **2000**, *104*, 4811.
(62) Zhao, Y.; Truhlar, D. G. *J. Phys. Chem. A* **2004**, *108*, 6908.
(63) Becke, A. D. *J. Chem. Phys.* **1993**, *98*, 1372.
(64) Staroverov, V. N.; Scuseria, G. E.; Tao, J.; Perdew, J. P. *J. Chem. Phys.* **2003**, *119*, 12129.
(65) Tao, J.; Perdew, J. P.; Staroverov, V. N.; Scuseria, G. E. *Phys. Rev. Lett.* **2003**, *91*, 146401.
(66) Krieger, J. B.; Chen, J.; Iafrate, G. J.; Savin, A. In *Electron Correlations and Materials Properties*; Gonis, A., Kioussis, N., Eds.; Plenum: New York, 1999, pp 463.
(67) Zhao, Y.; Lynch, B. J.; Truhlar, D. G. *Phys. Chem. Chem. Phys.* **2005**, *7*, 43.
(68) Boese, A. D.; Handy, N. C. *J. Chem. Phys.* **2002**, *116*, 9559.
(69) Zhao, Y.; Truhlar, D. G. *Theor. Chem. Acc.* **2008**, *120*, 215.
(70) Zhao, Y.; Truhlar, D. G. *Acc. Chem. Res.* **2008**, *41*, 157.
(71) Zhao, Y.; Schultz, N. E.; Truhlar, D. G. *J. Chem. Phys.* **2005**, *123*, 161103.
(72) Zhao, Y.; Truhlar, D. G. *J. Phys. Chem. A* **2005**, *109*, 5656.
(73) Zhao, Y.; González-García, N.; Truhlar, D. G. *J. Phys. Chem. A* **2005**, *109*, 2012.
(74) Boese, A. D.; Martin, J. M. L. *J. Chem. Phys.* **2004**, *121*, 3405.
(75) Zhao, Y.; Truhlar, D. G. *J. Chem. Theory Comput.* **2008**, *4*, 1849.
(76) Zhao, Y.; Schultz, N. E.; Truhlar, D. G. *J. Chem. Theory Comput.* **2006**, *2*, 364.
(77) Zhao, Y.; Truhlar, D. G. *J. Phys. Chem. A* **2006**, *110*, 13126.
(78) Heyd, J.; G. E. Scuseria, G. E.; Ernzerhof, M. *J. Chem. Phys.* **2003**, *118*, 8207.
(79) Henderson, T. M.; Izmaylov, A. F.; Scalmani, S.; Scuseria, G. E. *J. Chem. Phys.* **2009**, *131*, 044108.
(80) Yanai, T.; Tew, D. P.; Handy, N. C. *Chem. Phys. Lett.* **2004**, *393*, 51.
(81) Iikura, H.; Tsuneda, T.; Yanai, T.; Hirao, K. *J. Chem. Phys.* **2001**, *115*, 3540.
(82) Vydrov, O. V.; Scuseria, G. E. *J. Chem. Phys.* **2006**, *125*, 234109.
(83) Chai, J.; Head-Gordon, M. *J. Chem. Phys.* **2008**, *128*, 084106.
(84) Chai, J.; Head-Gordon, M. *Phys. Chem. Chem. Phys.* **2008**, *10*, 6615.
(85) Peverati, R.; Truhlar, D. G. *Phys. Chem. Chem. Phys.* **2012**, *14*, 16187.
(86) Peverati, R.; Truhlar, D. G. *J. Phys. Chem. Lett.* **2011**, *2*, 2810.
(87) Noodleman, L.; Han, W. G. *J. Biol. Inorg. Chem.* **2006**, *11*, 674.
(88) Görling, A. *Phys. Rev. A* **1993**, *47*, 2783.
(89) Philipsen, P. H. T.; Baerends, E. J. *Phys. Rev. B* **1996**, *54*, 5326.
(90) Johnson, E. R.; Becke, A. D. *Can. J. Chem.* **2009**, *87*, 1369.
(91) Seeger, R.; Pople, J. A. *J. Chem. Phys.* **1977**, *66*, 3045.
(92) Bauernschmitt, R.; Ahlrichs, R. *J. Chem. Phys.* **1996**, *104*, 9047.
(93) Gräfenstein, J.; Hjerpe, A. M.; Kraka, E.; Cremer, D. *J. Phys. Chem. A* **2000**, *104*, 1748.
(94) Nishino, M.; Yamanaka, S.; Yoshioka, Y.; Yamaguchi, K. *J. Phys. Chem. A* **1997**, *101*, 705.
(95) Yanagisawa, S.; Tsuneda, T.; Hirao, K. *J. Chem. Phys.* **2000**, *112*, 545.
(96) Peverati, R.; Truhlar, D. G. *Philos. Trans. R. Soc., A* online as of April 23, **2013**; http://arxiv.org/abs/1212.0944.
(97) Yang, K.; Zheng, J.; Zhao, Y.; Truhlar, D. G. *J. Chem. Phys.* **2010**, *132*, 164117.
(98) Korth, M.; Grimme, S. *J. Chem. Theory Comput.* **2009**, *5*, 993.
(99) Goerigk, L.; Grimme, S. *Phys. Chem. Chem. Phys.* **2011**, *13*, 6670.
(100) Grimme, S. *Wiley Interdiscip. Rev.: Comput. Mol. Sci.* **2011**, *1*, 211.
(101) Goerigk, L.; Kruse, H.; Grimme, S. *ChemPhysChem* **2011**, *12*, 3421.
(102) Grimme, S.; Mück-Lichtenfeld, C. *Israel J. Chem.* **2012**, *52*, 180.
(103) Zhao, Y.; Truhlar, D. G. *J. Chem. Phys. Lett.* **2011**, *502*, 1.
(104) Li, R.; Peverati, R.; Isegawa, M.; Truhlar, D. G. *J. Phys. Chem. A* **2013**, *117*, 169 and refs therein.
(105) Harvey, J. N. *Struct. Bonding (Berlin)* **2004**, *112*, 151.
(106) Perdew, J. P.; Wang, Y. *Phys. Rev. B* **1986**, *33*, 8800.
(107) Cooper, V. R. *Phys. Rev. B* **2010**, *81*, 161104.
(108) Kanneman, F. O.; Becke, A. D. *J. Chem. Theory Comput.* **2009**, *5*, 719.

(109) Murray, É. D.; Lee, K.; Langreth, D. C. *J. Chem. Theory Comput.* **2009**, *5*, 2754.
(110) Lee, K.; Murray, E. D.; Kong, L.; Lundqvist, B. I.; Langreth, D. C. *Phys. Rev. B* **2010**, *82*, 081101.